Chapter 1

ACCURATE NONLINEAR OPTICAL PROPERTIES FOR SMALL MOLECULES.

Methods and results

Ove Christiansen[1], Sonia Coriani[2], Jürgen Gauss[3], Christof Hättig[4], Poul Jørgensen[1], Filip Pawłowski[5], and Antonio Rizzo[6]

[1] *Department of Chemistry, University of Århus, Langelandsgade 140, DK-8000 Århus C, Denmark;* [2] *Dipartimento di Scienze Chimiche, Università degli Studi di Trieste, Via L. Giorgieri 1, I-34127 Trieste, Italy;* [3] *Institut für Physikalische Chemie, Universität Mainz, D-55099 Mainz, Germany;* [4] *Forschungszentrum Karlsruhe, Institute of Nanotechnology, P.O. Box 3640, D-76021 Karlsruhe, Germany;* [5] *Department of Chemistry, University of Oslo, P.O. Box 1033 Blindern, N-0315 Oslo, Norway;* [6] *Istituto per i Processi Chimico-Fisici del Consiglio Nazionale delle Ricerche, Area della Ricerca, via G. Moruzzi 1, loc. S. Cataldo, I-56124 Pisa, Italy;*

Abstract During the last decade it became possible to calculate by quantum chemical *ab initio* methods not only static but also frequency-dependent properties with high accuracy. Today, the most important tools for such calculations are coupled cluster response methods in combination with systematic hierarchies of correlation consistent basis sets. Coupled cluster response methods combine a computationally efficient treatment of electron correlation with a qualitatively correct pole structure and frequency dispersion of the response functions. Both are improved systematically within a hierarchy of coupled cluster models.

The present contribution reviews recent advances in the highly accurate calculation of frequency-dependent properties of atoms and small molecules, electronic structure methods, basis set convergence and extrapolation techniques. Reported applications include first and second hyperpolarizabilities, Faraday, Buckingham and Cotton–Mouton effects as well as Jones and magneto-electric birefringence.

Keywords: coupled cluster, CCSD, CC3, response theory, quasi-energy Lagrangian, time-dependent perturbation theory, frequency-dependent properties, hyperpolarizabilities, basis set convergence, magnetic optical rotation, magnetic circular dichroism, Verdet constant, Faraday effect, Buckingham effect, Cotton–Mouton effect, Jones birefringence, magneto-electric birefringence.

Introduction

The developments of laser technology have in the last decades made the field of nonlinear optics (NLO) increasingly important. Today lasers that produce light with well-defined properties and high intensities are in widespread use. In recent years it has become possible to generate in addition very strong magnetic fields. Thus a wealth of NLO processes that arise in the presence of strong static and dynamic electric and magnetic fields became accessible. Accordingly many modern experiments are related in one or the other way to NLO processes. Another motivation for studying NLO properties is the quest for new materials with specific NLO properties for creating new generations of optical devices. This quest has initiated a significant activity in the development of theoretical methods for describing NLO processes.

The theoretical prediction of NLO properties using high accuracy *ab initio* methods has been primarily focused on small molecules, where there has been a significant interplay between theory and experiment [1–39]. Among NLO properties, the interest in birefringences and their absorptive counterparts (dichroisms) has increased during the last decade with the progress in optics and detection techniques on the experimental side, and with the fast advance of methods and computational power from the theoretical side [40]. The interplay between theory and experiment has also been essential for illuminating the role of various physical effects in relation to NLO processes and for the design of molecules, chromophores, functional groups, etc., with specific NLO properties.

The calculation of NLO properties with high accuracy is challenging and requires consideration of many different issues. While electron correlation is known to be important for accurate predictions of essentially all molecular properties, it is often of extreme importance for NLO properties. Rather extensive one-electron basis sets must be used to obtain reasonably well-converged results. NLO properties are related to optical experiments with external frequencies different from zero. The calculation of frequency-dependent properties can nowadays be achieved in theoretical methods for example with the response theoretical approach [41–44] discussed in this review. However, it cannot easily be obtained via the finite field techniques that are often used in the calculation of static properties. Molecular vibrations also have a significant effect on NLO properties. They cause an averaging of the electronic contribution over the vibrational motion leading to a so-called zero-point vibrational (ZPV) correction to the electronic contribution calculated at the equilibrium geometry. For many NLO properties there are also significant pure vibrational contributions. We refer to later chapters of this book for a detailed discussion of these contributions.

Relativistic effects have also been considered. Though they may be important for heavier elements, we shall not discuss this issue in detail here, since most of the applications presented are for molecules containing only light atoms. Our review will focus on the prediction of electronic contributions to NLO properties of molecules in the gas phase discussing the above issues in relation to theory and to actual calculations on small molecules. It will be shown that with benchmark calculations it is nowadays possible to predict NLO effects with unprecedented accuracy in a variety of systems and in this way to assess the quality of experiments.

The *ab initio* calculation of NLO properties has been a topic of research for about three decades. In particular, response theory has been used in combination with a number of electronic structure methods to derive so-called response functions [41–48]. The latter describe the response of a molecular system for the specific perturbation operators and associated frequencies that characterize a particular experiment. For example, molecular hyperpolarizabilities can be calculated from the quadratic and cubic response functions using electric dipole operators. From the frequency-dependent response functions one can also determine expressions for various transition properties (e.g. for multi-photon absorption processes) and properties of excited states [42].

One of the advantages of response theory is that it can be applied for most quantum chemical methods, including Hartree-Fock self-consistent-field (HF-SCF) [42,45], multi-configurational SCF (MCSCF) [42,49,50], and coupled cluster (CC) [44,46,51]. In recent years density functional theory (DFT) based response theory [52,53] has also received considerable interest. Response theory based upon HF-SCF and DFT has the advantage of being applicable to rather large systems, but on the other hand is not always appropriate for detailed and quantitatively accurate comparisons with experiment. Since dynamic electron correlation is typically very important for the predictions of NLO properties efficient and accurate treatments of dynamic correlation are required for obtaining quantitative results. Due to the exponential parameterization and the accompanying correct scaling with the size of the system, CC methods have the possibility to give accurate results for systems with both few and many electrons as long as the calculations are feasible.

The high accuracy of CC methods is well established for a number of molecular properties including structures, vibrations, NMR shielding etc. In particular CC models with an approximate treatment of triple excitations as e.g. the CCSD(T) method [54] provide a high accuracy. Despite all its qualities there is an inherent problem in the use of CCSD(T) in relation to NLO properties: While static properties can be obtained with high accuracy using CCSD(T) the description of the frequency dependence is dubious within this approach. A similar problem holds for MP2. These methods have a frequency dependence that is corrupted by the presence of poles due to the HF-SCF reference state.

However, a hierarchy of CC methods has been developed [55–71] for the calculation of response properties including CC2 [57], coupled cluster singles and doubles (CCSD) [72], and CC3 [56,58], etc. The advantage of CC2 and CC3, as compared to MP2 and CCSD(T), is that they have a frequency dependence that matches the quality of the static properties. Thus in the CC2, CCSD and CC3 sequence both static and frequency-dependent molecular properties as well as electronic excitation energies are obtained with increasing accuracy at the cost of increasing computational effort. For these methods linear [60–64], quadratic [65–67] and cubic response functions [67,68] have been implemented and allow today accurate and systematic calculations of NLO properties including hyperpolarizabilities [30, 32, 36, 37, 73], magneto-optical effects [38, 39, 70, 71, 74], two-photon absorption [75, 76], and so on. In principle, the hierarchy of CC methods also extends further to the full coupled cluster singles, doubles and triples (CCSDT) method and beyond, but at this level the calculation begins to be too demanding using present day standards for computer equipment and such methods have been little used for the calculation of NLO properties besides benchmark studies [34, 39, 64, 77, 78]. On the other hand CC2 and in some cases even CCSD are not accurate enough for detailed studies of NLO properties of small molecules. The experience with CC3 has been that this is a very accurate method also for NLO properties. Indeed, CC3 is probably the most accurate methodology for frequency-dependent properties applicable nowadays to systems with more than a few electrons. In this paper the focus is on high accuracy NLO calculations and the role of CC3 is in this context extremely important since it often gives the final increase in accuracy that allows us to support, interpret, predict, or reject experimental results with confidence.

In the next section we summarize the theoretical background for coupled cluster response theory and discuss certain issues related to their actual implementation. In Sections 2 and 3 we describe the application of quadratic and cubic response in calculations of first and second hyperpolarizabilities. The use of response theory to calculate magneto-optical properties as e.g. the Faraday effect, magnetic circular dichroism, Buckingham effect, Cotton-Mouton effect or Jones birefringence is discussed in Section 4. Finally we give some conclusions and an outlook in Section 5.

1. Coupled cluster response theory

In standard time-independent coupled cluster theory the wavefunction is parameterized as

$$|\mathrm{CC}\rangle = \exp(\hat{T})|\mathrm{Ref}\rangle \ , \tag{1.1}$$

where $\hat{T} = \sum_\mu t_\mu \hat{\tau}_\mu$ is the cluster operator, $|\mathrm{Ref}\rangle$ a reference state—usually taken as the Hartree-Fock wavefunction $|\mathrm{HF}\rangle$—and $\hat{\tau}_\mu$ excitation operators [79] which applied to the reference state generate excited determinants or configura-

tions $|\Phi_\mu\rangle = \hat{\tau}_\mu|\mathrm{Ref}\rangle$. The amplitudes t_μ of the cluster operator are determined by projecting the Schrödinger equation onto the bra states $\langle\mathrm{Ref}|\hat{\tau}_\mu^\dagger \exp(-\hat{T})$:

$$0 = \left\langle \mathrm{Ref}\middle|\hat{\tau}_\mu^\dagger \exp(-\hat{T})\hat{H}\exp(\hat{T})\middle|\mathrm{Ref}\right\rangle \ , \tag{1.2}$$

and the energy is obtained as

$$E_{\mathrm{CC}} = \langle\mathrm{Ref}|\hat{H}|\mathrm{CC}\rangle \ . \tag{1.3}$$

By truncating the cluster operator $\hat{T}$ after single, double, triple, ... replacements the hierarchy of coupled cluster models CCS, CCSD, CCSDT, etc. is obtained. In this series the accuracy of the results—but also the computational costs—converge rapidly to those of Full Configuration Interaction (FCI). This motivated the development of several intermediate methods which are derived from the above standard models by either

- augmenting the CC energy of Eq. (1.3) with perturbative corrections (e.g. CCSD[T] [80,81], CCSD(T) [54], CCSDT(Q$_f$) [82], ...)
- or introducing approximations into the cluster equations (1.2) — (e.g. CC2 [57], CC3 [56], CCSDT-1a [83,84], ...)

For a detailed review of coupled cluster methods for ground state energies and static properties the reader is referred to Refs. [79,85–87].

1.1 Including a time-dependent perturbation

In response theory one considers a quantum mechanical system described by the time-independent Hamiltonian $\hat{H}^{(0)}$ which is perturbed by a time-dependent perturbation $\hat{V}(t,\epsilon)$

$$\hat{H}(t,\epsilon) = \hat{H}^{(0)} + \hat{V}(t,\epsilon) \ . \tag{1.4}$$

We assume that the perturbation $\hat{V}$ can be expanded in a sum over monochromatic Fourier components as

$$\hat{V}(t,\epsilon) = \sum_j \epsilon_j \ \exp(-i\omega_j t)\, \hat{X}_j \ , \tag{1.5}$$

where $\hat{X}_j$ are hermitian time-independent one-electron operators and ϵ_j are the amplitudes of the associated field-strengths. (The letter ϵ without index is above and in the following used as abbreviation for all field strengths $\{\epsilon_j\}$ included in $\hat{V}$.) We shall furthermore assume for simplicity that the perturbations in Eq. (1.5) have a common time period and that $\hat{V}$ is hermitian, which implies that for each frequency ω_j also its negative is included in the summation.

The time-dependent ground-state coupled cluster wavefunction for such a system is conveniently parameterized in a form, where the oscillating phase

factor caused by the so-called level-shift [43–45, 88, 89] or time-dependent quasi-energy $\mathcal{W}(t,\epsilon)$ (vide infra) is explicitly isolated [42–46, 90, 91]:

$$\Big|\overline{\mathrm{CC}}(t,\epsilon)\Big\rangle = \exp\Big(-i\int_{t_0}^{t}\mathcal{W}(t',\epsilon)dt'\Big)\Big|\mathrm{CC}(t,\epsilon)\Big\rangle \tag{1.6}$$

with

$$|\mathrm{CC}(t,\epsilon)\rangle = \exp(\hat{T}(t,\epsilon))|\mathrm{Ref}\rangle \ . \tag{1.7}$$

Note that in the time-independent limit $|\mathrm{CC}(t,\epsilon)\rangle$ becomes the usual time-independent CC wavefunction, Eq. (1.1), while the full time-dependent wavefunction $|\overline{\mathrm{CC}}(t,\epsilon)\rangle$ goes to $\exp\left(iE_{\mathrm{CC}}(t_0-t)\right)|\mathrm{CC}\rangle$. The reference state should be chosen such that it is time-independent—for the following it will be assumed that $|\mathrm{Ref}\rangle$ is the Hartree-Fock wavefunction of the unperturbed molecule $|\mathrm{HF}_0\rangle$. By keeping the uncorrelated reference state fixed in the presence of the perturbation, a two–step approach, which would introduce artificial poles into the correlated CC wavefunction due to the response of the orbitals, is avoided. Inserting the above ansatz into the time-dependent Schrödinger equation and projecting on the bra states $\langle\mathrm{HF}_0|\hat{\tau}_\mu^\dagger\exp(-\hat{T})$, the time-dependent cluster equations become

$$0 = \Big\langle\mathrm{HF}_0\Big|\hat{\tau}_\mu^\dagger\exp(-\hat{T})\hat{H}(t,\epsilon)\exp(\hat{T})\Big|\mathrm{HF}_0\Big\rangle - i\frac{d}{dt}t_\mu = e_\mu(t,\epsilon) - i\frac{d}{dt}t_\mu \ . \tag{1.8}$$

The energy, which in the time-dependent case is no longer a constant of motion, has to be generalized to the time-dependent quasi-energy:

$$\mathcal{W}(t,\epsilon) = \Big\langle\mathrm{HF}_0\Big|\exp(-\hat{T})\hat{H}(t,\epsilon)\exp(\hat{T})\Big|\mathrm{HF}_0\Big\rangle \ . \tag{1.9}$$

Frequency-dependent higher-order properties can now be obtained as derivatives of the real part[1] of the time-average of the quasi-energy $\{\mathcal{W}\}_T$ with respect to the field strengths of the external perturbations. To derive computational efficient expressions for the derivatives of the coupled cluster quasi-energy, which obey the $2n$+1- and $2n$+2-rules of variational perturbation theory [44, 45, 93], the (quasi-) energy is combined with the cluster equations to a Lagrangian:

$$L(t,\epsilon) = \mathcal{W}(t,\epsilon) + \sum_\mu \bar{t}_\mu\Big(e_\mu(t,\epsilon) - i\frac{d}{dt}t_\mu\Big) \tag{1.10}$$

[1]The imaginary part of $\mathcal{W}(t,\epsilon)$ is connected to the time derivative of the wavefunction norm and does not contain information about physical observables. For normalized wavefunctions and bra and ket state conjugated to each other the quasi-energy is real [44, 45]. However, the CC energy is calculated from a projection expression and in general not real. Thus with CC wavefunctions it is important to consider only the real part of the quasi-energy [44, 65, 92].

The time-average of the quasi-energy Lagrangian

$$\{L(t,\epsilon)\}_T = \lim_{t_0\to\infty} \frac{1}{2t_0} \int_{-t_0}^{+t_0} L(t,\epsilon)\, dt \ , \tag{1.11}$$

is required to be stationary with respect to the cluster amplitudes t_μ and the Lagrange multipliers $\bar{t}_\mu$ [43–45,48,88,94].

$$\delta\{L(t,\epsilon)\}_T = 0 \tag{1.12}$$

The last equation is a variation principle for the coupled cluster quasi-energy and wavefunction within oscillating harmonic external fields. If one inserts a perturbation and Fourier expansion as ansatz for the cluster amplitudes

$$\begin{aligned} t_\mu(t,\epsilon) &= t_\mu^{(0)} + \sum_{n=1}^{\infty} \frac{1}{n!} \sum_{j_1} \cdots \sum_{j_n} t_\mu^{X_{j_1}\ldots X_{j_n}}(\omega_{j_1},\ldots,\omega_{j_n}) \\ &\quad \times \prod_{m=1}^{n} \epsilon_{j_m}(\omega_{j_m}) \exp(-i\omega_{j_m} t) \ , \end{aligned} \tag{1.13}$$

and an analogous ansatz for the Lagrange multipliers Eq. (1.12) becomes a set of linear equations for the individual expansion coefficients of t_μ and $\bar{t}_\mu$, apart from the unperturbed cluster amplitudes, $t_\mu^{(0)}$, for which the nonlinear cluster equations, Eq. (1.2), are recovered. The response functions, i.e. the frequency-dependent higher-order properties, are obtained as derivatives of the real part of the time-dependent quasi-energy Lagrangian [44,65,92,95]:

$$\langle\langle X_1; X_2, \ldots, X_n\rangle\rangle_{\omega_2,\ldots,\omega_n} = \left(\frac{d^n \left\{ \frac{1}{2} L(t,\epsilon) + \frac{1}{2} L(t,\epsilon)^* \right\}_T}{d\epsilon_1(\omega_1)\ldots d\epsilon_n(\omega_n)} \right)_0 \ , \tag{1.14}$$

$$= \frac{1}{2} \hat{C}^{\pm} \left(\frac{d^n \{L(t,\epsilon)\}_T}{d\epsilon_1(\omega_1)\ldots d\epsilon_n(\omega_n)} \right)_0 \ , \tag{1.15}$$

where $\hat{C}^{\pm}$ symmetrizes with respect to an inversion of the signs of all frequencies and simultaneous complex conjugation[2]. Note that as a consequence of the time-averaging of the quasi-energy Lagrangian, the derivative in the last equation gives only a non-vanishing result if the frequencies of the external fields fulfill the matching condition $\sum_i \omega_i = 0$.

1.2 The issue of orbital relaxation

As pointed out above, in the time-dependent case the correlation treatment cannot be based on *time-dependent* Hartree-Fock orbitals—at least not on the

[2]The operator $\hat{C}^{\pm}$ is defined by $\hat{C}^{\pm} f(\omega_1,\omega_2,\ldots) = f(\omega_1,\omega_2,\ldots) + f(-\omega_1,-\omega_2,\ldots)^*$.

real frequency axis in the vicinity of poles of the response functions. Thus, the polarization of the wavefunction must be described through the variables of the correlations method, i.e. for the CC approach by means of the cluster amplitudes. This has important implications on the choice or suitability of correlation methods. As it is apparent from the sum-over-states expression for the n-th response function [96]

$$\begin{aligned}\langle\langle X_{n+1}; X_n, \ldots, X_1\rangle\rangle_{\omega_n,\ldots,\omega_1} &= \hat{P}^{X_{n+1}X_n\ldots X_1} \sum_{l_1\ldots l_n} \langle\Psi_0|\hat{X}_{n+1}|\Psi_{l_n}\rangle \\ &\times \prod_{m=1}^{n} \frac{\langle\Psi_{l_m}|\hat{X}_m|\Psi_{l_{m-1}}\rangle}{E_0 - E_{l_m} + \sum_{i=1}^{m}\omega_i} \quad , \quad (1.16)\end{aligned}$$

(where $\hat{P}^{X_{n+1}X_n\ldots X_1}$ is a symmetrization operator generating all possible permutations of the operators together with the accompanied frequencies and the summations are over all states Ψ_{l_m}) a qualitatively correct description requires up to $(n+1)/2$-tuple excitations, i.e. single excitations for linear and quadratic response functions, double excitations for cubic and quartic response functions and so on. To account simultaneously for dynamic correlation also at least the next two higher excitation levels need to be included, i.e. at least triple excitations for the linear and quadruple excitations for the cubic response function. These excitations are not necessarily connected and are therefore most efficiently parameterized via the exponential coupled cluster ansatz, Eq. (1.1). In

Table 1.1. Hierarchy of coupled cluster methods for response calculations. The table summarizes to which order in the electron fluctuation potential ground state and single excitation energies and response functions are obtained correctly at a given level of the correlation treatment. The analysis is based on a Møller-Plesset like partitioning of the Hamiltonian as $\hat{H}(t,\epsilon) = \hat{F} + \hat{U} + \hat{V}(t,\epsilon)$, where $\hat{U}$ is the electron fluctuation potential [58, 59].

method	scaling of comp. effort[a]	ground state energy[b]	single excitation poles	response functions
HF-SCF	$< N^4$ (iter.)	1	1	1
CCS	$< N^4$ (iter.)	1	1	0
MP2	nN^4	2	—	—
CC2	nN^4 (iter.)	2	2	1
CCSD	n^2N^4 (iter.)	3	2	2
CCSD(T)	n^3N^4	4	—	—
CC3	n^3N^4 (iter.)	4	3	3
CCSDT-1a/b	n^3N^4 (iter.)	4	2	2
CCSDT	n^4N^4 (iter.)	4	4	4

[a] n and N are, respectively, the number of electrons and basis functions, an addition (iter.) indicates that the highest cost appear in iterative steps. Given are the formal scaling without exploiting screening; the exact costs depend heavily on the implementation. [b] for the unperturbed system, i.e. no fields added after the HF calculation.

a configuration interaction (CI) picture, however, these high excitations need to be explicitly included. For this reason, truncated CI methods have never been applied very successfully for the calculation of frequency-dependent properties of many-electron systems, even though implementations have been reported in the literature [97–100].

Also for coupled cluster methods the use of unrelaxed orbitals has some implications. A perturbation theoretical analysis based on a Møller-Plesset like partitioning of the Hamiltonian as $\hat{H}(t,\epsilon) = \hat{F} + \hat{U} + \hat{V}(t,\epsilon)$, where $\hat{U}$ is the electron fluctuation potential and $\hat{F} + \hat{V}(t,\epsilon)$ is used as zeroth-order Hamiltonian, leads to the conclusion that in the presence of "unrelaxed" fields the results of coupled cluster methods are in general not correct through the same order in the fluctuation potential as they are in the absence of such fields [59]. Thus, CCSD, for example, gives response functions which are only correct through second order in $\hat{U}$, while CCSD ground state energies are correct through third order (compare Table 1.1). However, it is unclear how the loss of one order in perturbation theory affects the accuracy of the results. It is well established for static properties like dipole moments and polarizabilities that the orbital–relaxed and orbital–unrelaxed results differ substantially. But the results are sometimes on different sides of the FCI values, with deviations of similar magnitudes depending on the molecule and the CC model [34,39,77,101–103]. We shall return to this issue in the numerical studies in Secs. 3.2 and 4.3.

1.3 Implementation in quantum chemistry programs

The approach outlined above combines the calculation of response functions (i.e. of frequency-dependent properties) with the theory of analytic derivatives developed for static higher-order properties. In the limit of a static perturbation all equations above reduce to the usual equations for (unrelaxed) coupled cluster energy derivatives. This is an invaluable advantage for the implementation of frequency-dependent properties in quantum chemistry programs.

The CC response functions are conveniently expressed in terms of partial derivatives of $L(t,\epsilon)$ with respect to cluster amplitudes, Lagrange multipliers and field strengths, which are given for the lowest orders in Table 1.2. Assuming that all perturbations included in $\hat{V}(t,\epsilon)$ are described by one-electron operators and that the basis set does not depend on the external fields (as it would e.g. with so-called *gauge including atomic orbitals* (GIAOs) [71,104–108]) for example the quadratic response function is obtained as:

$$\begin{aligned}\langle\langle A;B,C\rangle\rangle_{\omega_B,\omega_C} &= \frac{1}{2}\hat{C}^{\pm\omega}\hat{P}^{ABC}\Big\{\frac{1}{6}\mathbf{G}\,t^A\,t^B\,t^C + \frac{1}{2}\mathbf{F}^A\,t^B\,t^C + \\ &\qquad \frac{1}{2}\bar{t}^A\,\mathbf{B}\,t^B\,t^C + \bar{t}^A\mathbf{A}^B\,t^C\Big\}\ .\end{aligned} \tag{1.17}$$

Table 1.2. Partial derivatives of the Lagrange functional for the coupled cluster quasi-energy

$\eta_\mu^{(0)} =$	$\left(\frac{\partial \mathcal{W}}{\partial t_\mu}\right)_{\epsilon=0}$	$A_{\mu\nu} =$	$\left(\frac{\partial^2 L}{\partial \bar{t}_\mu \partial t_\nu}\right)_{\epsilon=0}$
$F_{\mu\nu} =$	$\left(\frac{\partial^2 L}{\partial t_\mu \partial t_\nu}\right)_{\epsilon=0}$	$B_{\mu\nu\gamma} =$	$\left(\frac{\partial^3 L}{\partial \bar{t}_\mu \partial t_\nu \partial t_\gamma}\right)_{\epsilon=0}$
$G_{\mu\nu\gamma} =$	$\left(\frac{\partial^3 L}{\partial t_\mu \partial t_\nu \partial t_\gamma}\right)_{\epsilon=0}$	$\xi_\mu^X =$	$\left(\frac{\partial^2 L}{\partial \epsilon_X \partial \bar{t}_\mu}\right)_{\epsilon=0}$
$\eta_\mu^X =$	$\left(\frac{\partial^2 L}{\partial \epsilon_X \partial t_\mu}\right)_{\epsilon=0}$	$A_{\mu\nu}^X =$	$\left(\frac{\partial^3 L}{\partial \epsilon_X \partial \bar{t}_\mu \partial t_\nu}\right)_{\epsilon=0}$

In the above equation the operator $\hat{P}^{ABC}$ symmetrizes with respect to permutations of the perturbations A, B, and C together with the accompanied frequencies and $\hat{C}^{\pm\omega}$ is the symmetrization defined in Sec. 1.1. The first-order responses of the cluster amplitudes and Lagrange multipliers are denoted as, respectively, t^X and $\bar{t}^X$. In addition to these and the unperturbed cluster amplitudes $t^{(0)}$ also the zeroth-order Lagrange multipliers $\bar{t}^{(0)}$ are needed. All these parameters are obtained from linear so-called response equations in which the Jacobian $\mathbf{A}$ as stability matrix enters as a central object:

$$\bar{t}^{(0)}\mathbf{A} = -\eta^{(0)} \tag{1.18}$$

$$\Big[\mathbf{A} - \omega_X \mathbf{1}\Big] t^X(\omega_X) = -\xi^X \tag{1.19}$$

$$\bar{t}^X(\omega_X)\Big[\mathbf{A} + \omega_X \mathbf{1}\Big] = -\Big(\eta^X + \mathbf{F}\, t^X(\omega_X)\Big) \tag{1.20}$$

The above equations are relatively straightforward to implement in a "direct" way without explicitly setting up and storing the matrices (and higher-order tensors) $\mathbf{A}$, $\mathbf{F}$, $\mathbf{G}$, $\mathbf{A}^X$, etc. Only intermediates of at most the size of the cluster amplitudes—i.e. $(nN)^m$, where n is the number of electrons, N the number of basis functions and m the highest excitation level—need to be stored in memory or on disk. Actually, for some approximate CC models one can reduce this further, as we shall see in the following for the CC3 model.

1.4 The approximate triples model CC3

For nonlinear (magneto-) optical properties, calculations of an accuracy close to that of modern gas phase experiments require—similar to what has also been found for other properties like structures [79, 109], reaction enthalpies [79, 110, 111], vibrational frequencies [112, 113], NMR chemical shifts [114], etc.—at least an approximate inclusion of connected triple excitations in the wavefunction. This has been known for years now from calculations of static hyperpolarizabilities with the CCSD(T) approximation [9–13]. CCSD(T) accounts rather efficiently for connected triples through a perturbative correction

on top of CCSD. For the reasons pointed out in Sec. 1.1 CCSD(T) is, as a two–step approach, not suitable for the calculation of frequency-dependent properties. Therefore, the CC3 model has been proposed [56, 58] as an alternative to CCSD(T) especially designed for use in connection with response theory. CC3 is an approximation to CCSDT—alike CCSDT-1a and related methods—where the triples equations are truncated such that the scaling of the computational efforts with system size is reduced to $\mathcal{O}(n^3N^4)$ as for CCSD(T), but the iterative character of the method is kept. The CC3 response functions are correct through third order in the fluctuation potential.

An important aspect of CC3 and other approximate triples methods is that due to the approximations made in the triples equations, it is possible to avoid the storage of the triples parts of the cluster amplitudes and Lagrange multipliers. This is essential since otherwise the storage and not the CPU requirements would limit the applicability of these methods.

To reduce the storage requirements, however, a more complicated partitioned formulation must be used which exploits the particular simple structure of the triples equations and the diagonality of the triples–triples block of the Jacobian. It allows to express the triples parts of the cluster amplitudes and Lagrange multipliers in terms of the singles and doubles parts and to reformulate the ground state cluster equations and the response equations that have to be solved to calculate properties, into effective equations in the space spanned by just the single and double excitation manifolds. Thereby the storage of full sets of triples amplitudes on disk or in core memory can be avoided. Instead the triples parts are calculated whenever needed "on-the-fly" from the singles and doubles parts and some integral intermediates. However, in the orbital-unrelaxed response approach needed for frequency-dependent properties some partial derivatives of $L(t, \epsilon)$ that appear in the right-hand-side vectors (e.g. ξ^X, η^X, and $\mathbf{A}^X$) induce an off-diagonal coupling between the triples amplitudes or multipliers of different order in response. This leads in higher order to quite involved expressions and algorithms, in particular if the optimal formal scaling of the computational costs with $\mathcal{O}(n^4N^3)$ should be conserved, and eventually this coupling will limit the applicability of a fully partitioned formulation.

What gives CC3 special prominence in response calculations is that this method is the simplest CC wavefunction model that yields response functions correct through third order in the fluctuation potential [56, 58]. The first implementations of the linear and quadratic response functions at the CC3 level that exploit the partitioning to eliminate the storage requirements for triples amplitudes were reported by Christiansen, Gauss and Stanton [62, 66] based on the triples code of the ACES II program package [115]. While the iterative solution of the response equations with given right hand sides proceeded with $\mathcal{O}(\mathcal{N}^7)$ scaling, these authors allowed in some non-iterative terms for higher-order scalings of the computational costs to obtain a close to optimal performance for

small molecules. Hald *et al.* [63, 69] and Pawłowski *et al.* [67, 73] reported an alternative implementation of the linear and quadratic response functions of CC3 and a first implementation of the cubic response function which conserves strictly the $\mathcal{O}(\mathcal{N}^7)$ scaling of the CC3 model at the expense of somewhat larger costs for small molecules. The latter implementation is based on the integral-direct coupled cluster code [116, 117] included in the Dalton program [118].

2. Frequency-dependent first hyperpolarizabilities

The conceptually simplest NLO property is the electric first dipole hyperpolarizability β. Nevertheless, it is a challenging property from both the theoretical and experimental side, which is related to the fact that, as third-rank tensor, it is a purely anisotropic property. Experimentally this means that β in isotropic media (gas or liquid phase) cannot be measured directly as such, but only extracted from the temperature dependence of the third-order susceptibilities $\chi^{(3)}$. In calculations anisotropic properties are often subject to subtle cancellations between different contributions and accurate final results are only obtained with a carefully balanced treatment of all important contributions.

2.1 Basis set convergence

According to the $2n$+1-rule first hyperpolarizabilities require similar to the linear polarizabilities only the calculation of the first-order response of the wavefunction. Thus, the minimal basis set requirements for a qualitative correct description of β_{ijk} are similar to those for the components of the linear polarizability α_{ij}, i.e. for calculations at a correlated level the basis set should be at least of triple-ζ quality augmented with diffuse functions for a better description of the long range part of the electron density and its response. However, for the first hyperpolarizability the experimentally observed properties (in most cases $\beta_{||}$ or $\beta_{\perp}$) are anisotropic tensors and therefore usually more sensitive to the quality of the wavefunction than the isotropic polarizability $\bar{\alpha}$. Within the hierarchy of correlation-consistent basis sets [120–123] augmentation with a single set of diffuse functions (aug-cc-pVXZ) is often sufficient for the calculation of polarizabilities of polyatomic molecules [101, 123]. For hyperpolarizabilities, in particular for small molecules, the doubly-augmented basis sets (d-aug-cc-pVXZ) give much better convergence with the cardinal number X, while the addition of even more diffuse functions as in the t-aug-cc-pVXZ sets does not give any further systematic improvements (see Tab. 1.3).

2.2 Convergence with correlation treatment

The situation is somewhat different for the convergence with the wavefunction model, i.e. the treatment of electron correlation. As an anisotropic and nonlinear property the first dipole hyperpolarizability is considerably more sensi-

Table 1.3. Basis set convergence of first hyperpolarizabilities $\beta_{\|}$ (in a.u.) at the (unrelaxed) CCSD level. For FH, CO, and H_2O results are given for the static limit $\beta_{\|}(0)$, while for HCl the results are for $\beta_{\|}(-\omega,\omega,0)$ with $\omega = 0.072003$ a.u. (632.8 nm). In all calculations a frozen core approximation with the electrons in the $1s$ shells of non-hydrogen atoms kept inactive in the correlation and response calculations is employed.

basis	FH[a]	HCl[b]	CO[c]	H_2O[d]
aug-cc-pVDZ	−9.32	19.53	27.95	−16.27
aug-cc-pVTZ	−9.80	12.42	26.34	−18.40
aug-cc-pVQZ	−8.63	8.77	25.37	−18.02
aug-cc-pV5Z	−8.29	9.49	25.12	−18.24
d-aug-cc-pVDZ	−6.01	10.96	26.78	−14.09
d-aug-cc-pVTZ	−7.68	9.71	25.43	−17.73
d-aug-cc-pVQZ	−7.73	8.95	25.06	−18.07
d-aug-cc-pV5Z	−7.77	8.94	24.99	−18.11
t-aug-cc-pVDZ	−6.29		26.77	−16.02
t-aug-cc-pVTZ	−7.93	9.48	25.26	−18.48
t-aug-cc-pVQZ	−7.87		25.04	−18.28
q-aug-cc-pVDZ	−6.40		27.00	−15.94
q-aug-cc-pVTZ	−7.93	9.34	25.34	−18.50
q-aug-cc-pVQZ	−7.84			

[a] R_{FH} = 1.7328 bohr; Z axis points from F to H; Refs. [65, 119]. [b] R_{HCl} = 1.27455 Å; Z axis points is from H to Cl; Ref. [37] (including some previously unpublished numbers). [c] R_{CO} = 2.132 bohr; Z axis points from O to C; present work and Ref. [36]. [d] R_{OH} = 0.957 Å, ∠(HOH) = 104.5°; Z axis points from O to the center of mass; present work and Ref. [36].

tive to the correlation treatment than linear dipole polarizabilities. Uncorrelated methods like HF-SCF or CCS yield for $\beta_{\|}$ results which are for small molecules at most qualitatively correct. Also CC2 is for higher-order properties not accurate enough to allow for detailed quantitative studies. Thus the CCSD model is the lowest level which provides a consistent and accurate treatment of dynamic electron correlation effects for frequency-dependent properties. With the CC3 model which also includes the effects of connected triples the electronic structure problem for $\beta_{\|}$ seems to be solved with an accuracy that surpasses that of the latest experiments (vide infra).

Table 1.4. The first hyperpolarizability of CO (from Ref. [36], results in a.u.).

Method	$\beta_{\parallel}^{\mathrm{static}}$	$\beta_{\parallel}^{\mathrm{SHG}}(694.3\ \mathrm{nm})$
CCSD/d-aug-cc-pVQZ[a]	25.06	29.09
CC3/d-aug-cc-pVTZ[a]	27.15	31.91
CC3/d-aug-cc-pVQZ[a,b]	26.78	31.44
CCSD(T)[c]	23.5	27.00
experimental value[d]		30.2 ± 3.2

[a] Ref. [36]; R_{CO} = 2.132 bohr. [b] estimated from CC3/d-aug-cc-pVTZ and CCSD results. [c] Ref. [8] static CCSD(T) result with Sadlej POL basis; for $\beta_{\parallel}^{\mathrm{SHG}}$ scaled with HF-SCF dispersion. [d] Ref. [1] rescaled in Ref. [16].

2.3 Comparison with experiment: CO, H_2O, FH, and HCl

Carbon monoxide. Table 1.4 shows results from Ref. [36] for the static and the second harmonic generation hyperpolarizabilities $\beta_{\parallel}^{\mathrm{SHG}}$ of CO at 694.3 nm. The electronic contributions were obtained from CC3/d-aug-cc-pVTZ calculations carried out at $R_{\mathrm{CO}} = 2.132$ bohr. These were approximately corrected for remaining basis set errors by adding the difference between CCSD/d-aug-cc-pVQZ and CCSD/d-aug-cc-pVTZ results for the same frequency and internuclear distance. For CO the triples correction for $\beta_{\parallel}(0)$ is 1.72 a.u. or $\approx 6\ \%$. At a wavelength of 694.3 nm the triples correction is already 2.35 a.u. or $\approx 7\%$. Thus, there is in this case a notable triples effect on the frequency dispersion. Since there is no information available about correlation contributions beyond CC3, it is difficult to assess the accuracy of these results.

The experimental result for $\beta_{\parallel}^{\mathrm{SHG}}$ at 694.3 nm is 30.2 ± 3.2 a.u. [1, 16]. This is in good agreement with the best theoretical estimate for the electronic contribution (31.44 a.u.). However, a direct comparison of the two values is hampered by the fact that presently no results are available for the zero-point vibrational correction as well as for the pure vibrational contribution.

Water. The same approach leads for water, H_2O, at the equilibrium geometry of $R_{\mathrm{OH}} = 0.957$ Å and $\angle(\mathrm{HOH}) = 104.5^{\circ}$ to a best estimate of -21.28 a.u. for the electronic second harmonic generation hyperpolarizability $\beta_{\parallel}^{\mathrm{SHG}}$ at 694.3 nm [36]. Also in this case connected triples are essential to obtain quantitative accuracy (they amount to $\approx 4\%$), but have only a minor effect on the dispersion (0.01 a.u. at 694.3 nm). For both the zero-point vibrational (ZPV) correction and the pure vibrational contribution, there are results available from previous theoretical investigations at the HF-SCF [15], MCSCF [14] and MP2 [15] levels. It is difficult to judge which of these results, which differ considerably, are most accurate. Probably the MP2 results of Ref. [15] are most

Table 1.5. The first hyperpolarizability of H_2O (from Ref. [36], results in a.u.).

Method	$\beta_{\parallel}^{\mathrm{static}}$	$\beta_{\parallel}^{\mathrm{SHG}}(694.3\ \mathrm{nm})$
CCSD/d-aug-cc-pVQZ[a]	-18.07	-21.98
CC3/d-aug-cc-pVTZ[a]	-17.04	-21.02
CC3/d-aug-cc-pVQZ[a,b]	-17.38	-21.28
zero point vibr. correct.[c]		-0.95
pure vibr. contrib.[c]		-0.21
best theoretical estimate		-22.4
experimental value[d]		-22.0 ± 0.9

[a] Ref. [36]; R_{OH} = 0.957 Å, $\angle$(HOH) = 104.5° [b] estimated from CC3/d-aug-cc-pVTZ and CCSD results. [c] Ref. [15] MP2 results. ZPV correction was calculated for static limit. [d] Ref. [1] rescaled in Ref. [16].

consistent with the coupled cluster calculations. At this level the ZPV correction has been estimated to be of the order of -0.95 a.u. The pure vibrational contribution has been calculated to about -0.21 a.u. at a frequency of 0.07 a.u. This frequency corresponds roughly to the experimental wavelength of 694.3 nm. Adding the MP2 vibrational corrections to the coupled cluster result for the electronic hyperpolarizability one obtains as a best estimate for the final result at 694.3 nm a value of -22.4 a.u. This is in excellent agreement with the experimental result for $\beta_{\parallel}^{\mathrm{SHG}}$ of -22.0 ± 0.9 a.u. reported in Refs. [1, 16] for this wavelength.

A comparison with an experimental result for a wavelength of 1064 nm of -19.2 ± 0.9 a.u. [17] is limited by missing data for the pure vibrational contribution at this wavelength. However, the best estimate for the electronic contribution including the aforementioned MP2 value for the ZPV correction obtained in Ref. [36] is with -19.81 a.u. in agreement with the experimental value.

Hydrogen fluoride. A somewhat special case is $\beta_{\parallel}^{\mathrm{SHG}}$ of hydrogen fluoride (FH). Since its experimental determination by Dudley and Ward [7] about twenty years ago and its first *ab initio* investigation by Sekino and Bartlett [13], there has been a discussion in the literature whether the experimental result is in agreement with theory or not [8,13,16,18,26–28,31,33,65,66,124]. However, both the experimental and the calculated results have relatively large uncertainties of 5 – 10%. For the theoretical value the main source of uncertainty are the vibrational contributions. The electronic contribution is today known with good accuracy from CC3 calculations [66] in a t-aug-cc-pVTZ basis and estimates for the remaining basis set error from CCSD calculations in large basis sets [65,119] and for higher-order correlation effects from FCI calculations [34]

Table 1.6. Second harmonic generation hyperpolarizability $\beta_{\parallel}^{\mathrm{SHG}}$ of FH at 694.3 nm (in a.u.).

	$\beta_{\parallel}^{\mathrm{SHG}}(694.3\ \mathrm{nm})$
CC3/t-aug-cc-pVTZ[a] at R_e	-8.32
est. remaining basis effects[b]	$+0.16 \pm 0.1$
est. remaining correl. effects[c]	$+0.07 \pm 0.1$
zero point vibr. correct.[d,e]	-0.72 ± 0.1
pure vibr. contrib.[e]	-0.64 ± 0.2
best theoretical estimate	-9.45 ± 0.5
experimental value[f]	-10.9 ± 1.0

[a] Ref. [66], R_e = 1.7328 bohr. [b] diff. between CCSD/d-aug-cc-pV5Z and CCSD/d-aug-cc-pVTZ, Refs. [65, 119]. [c] diff. between CC3/aug-cc-pVDZ and FCI/aug-cc-pVDZ, Ref. [34]. [d] diff. between vibrational averaged and single point (at R_{FH} = 1.7328 bohr) results, Ref. [119]. [e] calculated with CCSD/t-aug-cc-pVTZ frequency-dependent properties and a CCSD(T)/t-aug-cc-pVTZ potential, Ref. [119]. [f] Ref. [7] based on CF_4 as reference.

in the aug-cc-pVDZ basis. The zero-point vibrational correction and the pure vibrational contributions have been calculated from (unrelaxed) CCSD/t-aug-cc-pVTZ results for the property curves and a potential energy curve evaluated at the CCSD(T)/t-aug-cc-pVTZ level [119]. Combining these results, one arrives for $\beta_{\parallel}^{\mathrm{SHG}}(694.3\ \mathrm{nm})$ at a best estimate of -9.45 ± 0.5 a.u., as shown in Table 1.6. This estimate includes for the remaining correlation and basis set errors an uncertainty of 0.2 a.u. and for the ZPV correction and the pure vibrational contributions uncertainties of, respectively, 0.1 and 0.2 a.u.

The experimental value is with -10.9 ± 1.0 a.u. somewhat larger, but has also a relatively large uncertainty of $\approx 10\%$. It is thus difficult to conclude from these numbers that there exists a significant disagreement between the experimental and theoretical results. However, as suggested previously, an experimental reinvestigation of $\beta_{\parallel}^{\mathrm{SHG}}$ for FH, would be needed to resolve the remaining discrepancy, in particular since the measurement of Ref. [7] was carried out with CF_4 as reference gas, for which the second hyperpolarizability is not known very accurately.

Hydrogen chloride. For hydrogen chloride a very similar approach results in considerably better agreement between the experimental and the *ab initio* calculated result. The electronic contribution has been obtained from calculations at the CC3/d-aug-cc-pVTZ level supplemented by CCSD/d-aug-cc-pV5Z for remaining basis set effects. The ZPV correction and the pure vibrational contributions were calculated from CC3/d-aug-cc-pVTZ results for the properties and a CCSD(T)/aug-cc-pVQZ potential energy curve. The final best estimate obtained in Ref. [37] for $\beta_{\parallel}^{\mathrm{SHG}}(694.3\ \mathrm{nm})$ by combining these

Table 1.7. Second harmonic generation hyperpolarizability $\beta_{\parallel}^{\mathrm{SHG}}$ of HCl at 694.3 nm (in a.u.).

	$\beta_{\parallel}^{\mathrm{SHG}}(694.3\ \mathrm{nm})$
CC3/d-aug-cc-pVTZ[a] at R_e	9.84
est. remaining basis effects[b]	-0.94
zero point vibr. correct.[c]	-0.16
pure vibr. contrib.[d]	$+0.4$
best theoretical estimate	9.14
experimental value[e]	9.76 ± 0.96

[a] Ref. [37], R_{HCl} = 1.27455 Å. [b] diff. between CCSD/d-aug-cc-pV5Z and CCSD/d-aug-cc-pVTZ, Ref. [37]. [c] static result from CC3/d-aug-cc-pVTZ property and CCSD(T)/aug-cc-pVQZ potential, Ref. [37]. [d] from CC3/d-aug-cc-pVTZ frequency-dependent properties and CCSD(T)/aug-cc-pVQZ potential, Ref. [37]. [e] Ref. [7] based on CF_4 as reference gas.

results is with 9.14 a.u. in very good agreement with the experimental value of 9.76 ± 0.96 a.u. from Ref. [7].

3. Frequency-dependent second hyperpolarizabilities

Naively, one would expect that second hyperpolarizabilities γ are theoretically and experimentally more difficult to obtain than first hyperpolarizabilities β. From a computational point of view the calculation of fourth-order properties requires, according to the $2n$+1-rule, second-order responses of the wavefunction and thus the solution of considerably more equations than needed for β (cf. Sec. 1.3). However, unlike β the second dipole hyperpolarizability γ has two isotropic tensor components ($\gamma_{\parallel}$ and $\gamma_{\perp}$) which are amenable to very accurate gas phase measurements [2–6,16,29] on atoms and small and highly symmetric molecules for which also very accurate calculations can be carried out.

3.1 Basis set convergence

Since second hyperpolarizabilities depend in addition to the first-order also on the second-order response of the wavefunction, the minimal requirements with respect to the choice of basis sets are for γ somewhat higher than for the linear polarizabilities α and the first hyperpolarizabilities β, in particular for atoms and small molecules. For the latter at least doubly-polarized basis sets augmented with a sufficient number of diffuse functions (e.g. d-aug-cc-pVTZ or t-aug-cc-pVTZ) are needed to obtain qualitatively correct results. Highly accurate results at a correlated level will in general only be obtained in quadruple-ζ or better basis sets.

Table 1.8 shows the results of basis set studies for the static isotropic second hyperpolarizabilities of Ne, N_2, and CH_4. These numbers illustrate the typical

Table 1.8. Basis set convergence of $\gamma_{\|}(0)$ (in a.u.) in HF-SCF and (unrelaxed) CCSD.

Basis Set	HF-SCF			CCSD		
	Ne[a]	N_2[b]	CH_4[c]	Ne[a]	N_2[b]	CH_4[c]
aug-cc-pVDZ	20.3	456	1497	29.6	684	1931
aug-cc-pVTZ	28.3	560	1745	42.2	745	2199
aug-cc-pVQZ	38.6	654	1830	58.5	822	2285
aug-cc-pV5Z	50.1	685		76.8	844	
d-aug-cc-pVDZ	49.3	672	1774	83.9	938	2328
d-aug-cc-pVTZ	57.3	697	1868	94.2	895	2364
d-aug-cc-pVQZ	62.0	710	1864	100.2	881	2330
d-aug-cc-pV5Z	67.5	714		108.0	873	
d-aug-cc-pV6Z	68.6	714			869	
t-aug-cc-pVDZ	53.2	669	1815	94.4	935	2378
t-aug-cc-pVTZ	66.5	710	1869	110.3	903	2365
t-aug-cc-pVQZ	67.8	713	1868	110.0	883	
t-aug-cc-pV5Z	68.6	714		110.2	873	
t-aug-cc-pV6Z	68.9	715		110.0		
q-aug-cc-pVDZ	53.3	680	1816	94.5	943	2380
q-aug-cc-pVTZ	68.9	717	1871	114.5	909	
q-aug-cc-pVQZ	68.5	715		111.2	884	
q-aug-cc-pV5Z	68.7			110.2		
q-aug-cc-pV6Z	68.9			110.0		
limit	68.8	715				

[a] Refs. [32, 119], CCSD calculations with frozen core approximation for $1s$ shell. [b] R_{NN} = 2.074 bohr; Refs. [32, 35]. [c] R_{CH} = 2.052 bohr; Refs. [32], CCSD calculations with frozen core approximation for $1s$ shell at C.

basis set convergence of this property, which apart from the higher minimal needs, resembles that of the isotropic polarizability $\bar{\alpha}$. As observed before by other authors [123], the results converge slowly with the cardinal number (or ζ-level) if the augmentation level is low. This reflects the important role of diffuse functions for these properties. For atoms (as Ne) one obtains both at the HF-SCF and at the correlated level an acceptable convergence first in the triply-augmented series t-aug-cc-pVXZ. The fourth set of diffuse functions improves slightly the convergence, but for correlated calculations an increase in the cardinal number X is more important. For molecules the basis set convergence is somewhat faster, in particular with respect to diffuse functions. For N_2 and CH_4 already in the doubly-augmented series an increase of the cardinal number X is of the same importance as triply augmentation.

At the Hartree-Fock level the hyperpolarizabilities usually increase if the augmentation level and also if the cardinal number X are increased. For the correlated contribution to $\gamma_{||}(0)$ the convergence pattern is dominated by differ-

Table 1.9. Convergence of $\gamma_{||}(0)$ with the wavefunction model. The basis sets are for Ne and Ar t-aug-cc-pV5Z and for N_2 and CH_4 t-aug-cc-pVTZ for HF-SCF, CCS and CC2 and d-aug-cc-pVTZ for CCSD and CCSD(T). Coupled cluster results with frozen–core approximation[3] with the exception of Ne and Ar, where all–electron CCSD(T) and CC3 results are given. Where not stated otherwise, the results are taken from Ref. [32].

	orbital–relaxed			orbital–unrelaxed			
	HF-SCF	CCSD	CCSD(T)	CCS	CC2	CCSD	CC3
Ne	68.6	99.1	107.1	78.2	135.8	110.2	108.0[b]
Ar	961	1106	1159	1154	1247	1178	1172[c]
N_2	710	854	911	825	992	895	
CH_4	1869	2176	2294	2228	2557	2364	

[b] Ref. [73]. [c] Ref. [125].

ent effects: At the CCSD level an increase of $\gamma_{||}(0)$ with the cardinal number beyond T is only found for the lower augmentation levels. In particular for molecules we observe, as illustrated in Table 1.8 for N_2 and CH_4, a monotonic decrease of the second hyperpolarizability when the correlation treatment is improved in the series X = T, Q, 5, etc. The results for X = T typically overestimate $\gamma_{||}(0)$ by a few percent. Many correlated hyperpolarizability calculations in the literature were performed with basis sets of triple-ζ or similar quality and basis set convergence was often only explored with respect to augmentation with diffuse functions. From the above observations one may conclude that many of these studies obtained too large results for $\gamma_{||}(0)$.

3.2 Convergence with correlation treatment

Coupled cluster response calculations are usually based on the HF-SCF wavefunction of the unperturbed system as reference state, i.e. they correspond to so-called orbital-unrelaxed derivatives. In the static limit this becomes equivalent to finite field calculations where the perturbation is added to the Hamiltonian after the HF-SCF step, while in the orbital-relaxed approach the perturbation is included already in the HF-SCF calculation. For frequency-dependent properties the orbital-relaxed approach leads to artificial poles in the correlated results whenever one of the involved frequencies becomes equal to an HF-SCF excitation energy. However, in the static limit both unrelaxed and relaxed coupled cluster calculations can be used and for both approaches the hierarchy CCS (HF-SCF), CC2, CCSD, CC3, ... converges in the limit of a complete cluster expansion to the Full CI result[3]. Thus, the question arises, whether for second

[3] Note that if a frozen core approximation is used a small difference will persist in the Full CI limit since the unrelaxed series converges to a limit with the core orbitals constrained to be those of the unperturbed

hyperpolarizabilities one of the two approaches is superior, i.e., converges faster to the FCI limit. A theoretical analysis of the response functions [59] based on a Møller-Plesset like partitioning of the Hamiltonian indicates that the unrelaxed hierarchy converges at least initially slower. It is therefore sometimes assumed in the literature that the orbital-relaxed hierarchy is more reliable [31,126,127], although numerical investigations [34,77,102,103] on small molecules do not support this supposition.

In order to compare the performance of the relaxed and unrelaxed hierarchies for second hyperpolarizabilities, the static limit $\gamma_{||}(0)$ has been calculated for Ne, Ar, N_2, and CH_4 using relaxed HF-SCF, CCSD and CCSD(T) and unrelaxed CCS, CC2, CCSD and CC3 (see Table 1.9). The lowest levels, HF-SCF and CCS, give results of similar accuracy, although the CCS values are somewhat higher and for all these cases between the HF-SCF and the correlated results. This indicates that the singles excitation manifold in the cluster expansion can account implicitly for most of the orbital relaxation effects. CC2 overestimates the correlation contributions to response properties and does not improve systematically upon HF-SCF and CCS—most likely a consequence of the fact that CC2 response functions are, as the HF-SCF ones, only correct through first order in the electron-electron interaction. This effect is less severe for (orbital-relaxed) MP2, which usually gives quite good results for second hyperpolarizabilities [8,11,16,123], but this method cannot be used in the unrelaxed response approach needed for frequency-dependent properties. At the CCSD level the unrelaxed results have errors which are by a factor 2 to 4 smaller than those obtained with orbital-relaxed CCSD, which, similar as HF-SCF, systematically underestimates isotropic hyperpolarizabilities. This has also been observed for other molecules and (isotropic) properties [34,55,59,128–130] and it seems to be a common trend. After including the effects of connected triple excitations at the CCSD(T) or CC3 level, the differences between the relaxed and unrelaxed approaches are small and, in the basis set limit, both provide results close to experimental accuracies. Thus, there is no indication that the implicit treatment of orbital relaxation via the singles and higher cluster excitations impairs the accuracy of coupled cluster response methods compared to the calculation of orbital-relaxed derivatives.

3.3 Comparison with experiment: Ne and N_2

Neon. The ESHG hyperpolarizability of Ne has been the subject of several experimental investigations and numerous *ab initio* calculations. The "ups" and "downs" of the theoretical and experimental estimates for γ_0^{Ne} have

system whereas in the relaxed series the relaxation contribution of the core orbitals is included. For electric (hyper)polarizabilities this effect is usually negligible.

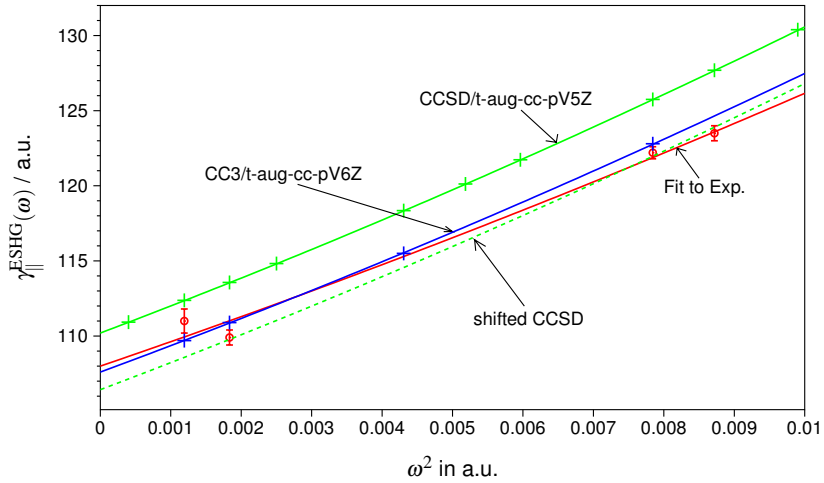


Figure 1.1. Electric field induced second harmonic generation in neon. Comparison of the CCSD and CC3 results from Ref. [73] with the experimental data from Refs. [6, 23]. For "shifted CCSD" the dispersion curve obtained with CCSD has been shifted to match best the experimental points for the two highest frequencies.

been described in detail in reviews by Bishop [24], Shelton and Rice [16] as well as in recent work by Hättig and Jørgensen [32] and Pawłowski, Jørgensen and Hättig [73]. After the latest ESHG experiments by Shelton and Donley [23], measurements at four frequencies were presumed to be accurate within $\pm 0.4 - 0.8$ au. A fit of the expression $\gamma_{\parallel}^{\mathrm{ESHG}}(\omega) = \gamma_0(1 + 6A\omega^2 + 36B\omega^4)$ to these four points with B constrained to 5.50 au (a value arbitrarily chosen between the results of a MP2 [12, 25] and a CASSCF [19] calculation) led for γ_0^{Ne} to an estimate of 108 ± 2.2 au. However, the dispersion curve obtained by this fit does not overlap with the error bars of the two ESHG measurements at 1319 and 1064 nm (see Fig. 1.1). As already pointed out by Shelton and Donley [23], this indicated that one of these two points has a larger error than conveyed by its statistical uncertainty. From the available data it was not possible to determine which of the two points is inaccurate.

A CCSD response calculation in a large basis set for the ESHG dispersion curve [30] showed that the inaccurate point is the one at 1319 nm. A revised extrapolation based on the CCSD dispersion curve led to a new static limit of $\gamma_0^{\mathrm{Ne}} = 106.4 \pm 2.2$ au.

In Ref. [73] the non-relativistic CC3 basis set limit of γ_0^{Ne} was determined to 107.0 ± 0.4 au. The corresponding CCSD(T) value is about 0.8 au smaller. For the first-order relativistic correction to γ_0^{Ne} Klopper *et al.* [131] obtained at the CCSD(T)/q-aug-cc-pCV6Z level a value of 0.59 a.u. The largest uncertainty in the calculations is presently due to correlation effects beyond CC3, since

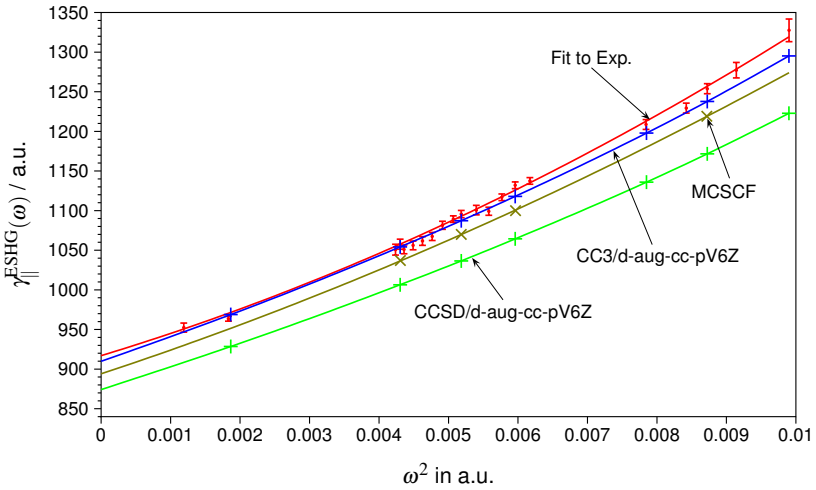


Figure 1.2. Electric field induced second harmonic generation in nitrogen N_2 (in a.u.). Comparison of the CCSD [32] and CC3 [35] results with a previous MCSCF calculation [20] and the experimental data from Refs. [2,3,6].

FCI calculations are only possible in small basis sets. The best available FCI result [125] for γ_0^{Ne}, calculated in a d-aug-cc-pVDZ basis, is -0.17 a.u. below the corresponding CC3 value. It is not known how well this result reproduces the basis set limit of the higher-order correlation contributions and we include therefore in our best estimate an uncertainty of 0.6 a.u. Adding the relativistic and the FCI$-$CC3 correction to the CC3 results leads to a best estimate for γ_0^{Ne} of 107.4 ± 1.0 a.u. in good agreement with the value extrapolated from the experimental results (106.4 ± 2.2 a.u.). For a comparison with the frequency-dependent experimental results see Fig. 1.1.

Nitrogen. For this molecule, ESHG measurements are available for a much larger number of frequencies. Thus, there is little doubt about the accuracy of the experimental values and a dispersion curve could be fitted to the measured data (corrected for rovibrational contributions) without referring to calculated dispersion coefficients [2,3,6].

For N_2, there is a sizeable triples contribution to the lowest dipole allowed excitation energy of about 0.07 eV or 0.7%. As a consequence of this (unrelaxed) CCSD underestimates the absolute value of the isotropic hyperpolarizability and its dispersion. The electronic contribution to the static limit $\gamma_0^{\mathrm{N_2}}$ has been calculated at the CCSD/t-aug-cc-pVTZ level [32] to be 903.0 a.u. However, as indicated above, the triple-ζ level is often too low for the calculation of second hyperpolarizabilities and the $\gamma_0^{\mathrm{N_2}}$ obtained at the CCSD/t-aug-cc-pVTZ level turned out to be about 40 a.u. above the CCSD basis-set limit result. The latter

has been calculated to be 863.3±3.3 a.u. [35]. Before comparing this result to the value extrapolated from experimental results, it has to be corrected for the ZPV contribution, which has been obtained in Ref. [32] to 12.0 a.u., thereby yielding 875.3±3.3 a.u. as the best estimate for the electronic contribution to $\gamma_0^{\mathrm{N}_2}$ at the CCSD level. Shelton [6] obtained an experimental value of $\gamma_0^{\mathrm{N}_2}$, 917±9 a.u., from the extrapolation of the results in Ref. [2] corrected for the pure rotational and vibrational contributions. The discrepancy between this experimental value and the CCSD best estimate is as large as 42 a.u. and makes very clear the importance of the triples contribution.

After inclusion of connected triples at the CC3 level and accounting for the zero-point vibrational contribution at this level and for remaining basis set effects, a theoretical value of 912.9±4.3 a.u. is obtained as best estimate for the electronic $\gamma_0^{\mathrm{N}_2}$ [35]. The latter value is in excellent agreement with the value of 917±9 a.u. extrapolated from the ESHG experiments [6].

A comparison of the CCSD and CC3 results obtained in the d-aug-cc-pV6Z basis with the experimental results is shown in Fig. 1.2. While the CCSD results for $\gamma_{\parallel}^{\mathrm{ESHG}}(\omega)$ differ from the experimental results typically by 6-8%, the CC3 results are generally in perfect agreement with experiment. Only for the highest frequencies the deviations become larger than the error bars of the measurements. These deviations are attributed mainly to remaining correlation effects, which are enhanced for the highest frequencies. The relativistic contribution to $\gamma_{\parallel}^{\mathrm{ESHG}}(\omega)$ of N_2 is small (about 1.0 a.u.) [35].

4. Mixed electric and magnetic properties: birefringences and dichroisms

In the previous section we discussed pure electric–dipole hyperpolarizabilities, in particular second harmonic generation. Another important class of NLO processes includes birefringences and dichroisms which can be rationalized (at least to lowest orders in perturbation theory) in terms of response functions involving, besides the electric–dipole, also magnetic–dipole and electric–quadrupole operators. Prominent examples related to quadratic response functions are

- magneto-optical activity (MOA). It comprises two effects, both originating from a differential interaction of the right and left circularly polarized components of linearly polarized light with matter due to the presence of a magnetic field parallel to the direction of propagation. The first is the magnetic optical rotation (MOR, also known as Faraday effect) [21], i.e. an induced rotation of the plane of polarization (or circular birefringence). The other is an induced circular dichroism referred to as magnetic-circular dichroism (MCD) [21, 22, 132, 133].

- electric-field gradient (EFG) induced birefringence, also known as Buckingham effect (BE). This birefringence is observed when linearly polarized light interacts with matter in the presence of an electric-field gradient [134, 135]. The relationship with MOA and in particular MOR will be discussed later.

Examples of NLO processes that involve also cubic response functions are:

- Cotton-Mouton effect (CME) [136, 137], the linear birefringence which arises in a sample with a magnetic induction field perpendicular to the linearly polarized light beam. The CME is the magnetic analogue of the Kerr effect (KE) [138,139] which describes the birefringence induced by an electric field. The optical axes in CME are the same as in the magneto-electric birefringence (MEB), the latter being observed in the presence of both an electric and a magnetic field perpendicular to each other and to the direction of propagation. In experimental investigations, the three birefringences usually superimpose, but their effects can be separated via their different dependences on the field strengths, i.e., KE $\propto E^2$, CME $\propto B^2$, and MEB $\propto EB$.

- Jones birefringence (JB) [140–143]: this birefringence is observed when linearly polarized light traverses a sample in the presence of both an electric and a magnetic field perpendicular to the direction of propagation but (unlike in the case of MEB) parallel to each other. The theoretical expression for JB is identical to that for MEB, but it should be noted that the two effects correspond to different experiments with the optical axes in the JB directed at $\pm 45^\circ$ with respect to those of the other three birefringences (KE, CME and MEB).

In the following, we will discuss how these effects can be investigated using quantum chemical methods and present results from high-level *ab initio* calculations that have been reported in the last few years.

An important issue for optical processes that involve a magnetic field as perturbation is the possible gauge-dependence of the results when obtained by means of approximate quantum chemical calculations. The dependence on the chosen origin for the vector potential (usually termed in the quantum chemical community the gauge-origin dependence) is unphysical and entirely due to the approximations imposed on the calculations (in particular, but not only, the use of finite one-electron basis sets). In many cases, the gauge-origin dependence can successfully be dealt with by using explicitly magnetic-field dependent basis functions such as the gauge-including atomic orbitals (GIAOs, also known as London atomic orbitals (LAOs)) [104,105,144]. However, some complications arise in the coupled-cluster treatment for frequency-dependent properties. Straightforward solutions to the gauge-origin problem are here only

possible if the corresponding response functions can be written as derivatives of lower-order response functions with respect to the applied magnetic field components (for a detailed discussion, see Ref. [71]).

4.1 Magneto-optical activity

The key quantity for the Faraday effect [21, 145, 146] is the Verdet constant [147] $V(\omega)$ which for molecules in the gas phase is given by

$$V(\omega) \propto i\varepsilon_{\alpha\beta\gamma}\langle\langle\hat{\mu}_\alpha;\hat{m}_\beta,\hat{\mu}_\gamma\rangle\rangle_{0,\omega}\ , \tag{1.21}$$

i.e., as the isotropic average over mixed electric- and magnetic-dipole quadratic response function components. In Eq. (1.21), $\varepsilon_{\alpha\beta\gamma}$ denotes the Levi-Civita tensor and $\hat{\mu}$ and $\hat{m}$ indicate the electric dipole and magnetic dipole operators, respectively.

MCD is quantitatively analyzed in terms of three magnetic rotatory strengths, the so-called Faraday A, B, and C terms [21]. The B terms are particularly important for detecting hidden transitions, even though they are in general small and difficult to measure [148]. Therefore, theoretical determinations of MCD may play an important role for a correct interpretation of experimental data. For a transition between the states a and j, the B term is given as the residue of the quadratic response function entering $V(\omega)$ in Eq. (1.21), i.e.

$$B\,(a \rightarrow j) \propto i\varepsilon_{\alpha\beta\gamma}\Big[\lim_{\omega\rightarrow\omega_{aj}}(\omega-\omega_{aj})\langle\langle\hat{\mu}_\gamma;\hat{m}_\beta,\hat{\mu}_\alpha\rangle\rangle_{0,\omega}\Big]\ , \tag{1.22}$$

with $\hbar\omega_{aj}$ as the corresponding transition energy.

Basis set convergence: MOA. Verdet constants have been investigated in Refs. [74] and [38] for a few centro-symmetric molecules using coupled-cluster response-theory techniques. For atoms, corresponding results can be found in Ref. [149].

The basis set convergence in the calculations of $V(\omega)$ is illustrated by discussing H_2 for which the CCSD calculations yield FCI results [74]. As seen from Table 1.10 addition of diffuse functions is essential to obtain reliable results. With the first augmentation level (aug-cc-pVXZ), convergence within 3 decimals is obtained at the quadruple- and quintuple-ζ level. Doubly- and triply augmentation on the other hand barely affect the results with remaining changes in the order of less than 0.1%. Comparison with the explicitly-correlated results from Bishop and Cybulski [150] proves the "benchmark" quality of the corresponding CCSD results. It is also worth noting that the basis set convergence is more or less independent of the frequency.

For other molecules (nitrogen N_2, acetylene (C_2H_2), and methane (CH_4)), the basis set studies from Ref. [74] indicate again the importance of diffuse functions. However, compared to H_2, it is found that the second augmentation

Table 1.10. FCI Verdet constants (a.u. $\times 10^7$) for H_2 at four different frequencies.[a]

Basis Set	ω (au)			
	0.11391	0.08284	0.06509	0.05360
cc-pVQZ	0.22640	0.11607	0.07070	0.04761
aug-cc-pVQZ	0.45643	0.22998	0.13912	0.09335
d-aug-cc-pVQZ	0.45679	0.23002	0.13911	0.09334
t-aug-cc-pVQZ	0.45665	0.22995	0.13907	0.09331
cc-pV5Z	0.28236	0.14421	0.08773	0.05903
aug-cc-pV5Z	0.45597	0.22965	0.13887	0.09319
d-aug-cc-pV5Z	0.45562	0.22944	0.13876	0.09310
Ref. [150][b]	0.45556	0.22946	0.13877	0.09312
Ref. [150][c]	0.50527	0.25361	0.15316	0.10270
Exp. [151]	0.501	0.251	0.150	0.103

[a] From Ref. [74]. [b] Explicitly correlated results at equilibrium geometry. [c] Rovibrationally and thermally averaged values

is slightly more important, while for a sufficiently large valence basis set the effects due to triply augmentation are almost negligible.

Convergence with electron correlation treatment: MOA. The convergence with respect to the electron correlation treatment has been analyzed in Ref. [74] for N_2, C_2H_2, and CH_4 using the CCS, CC2, CCSD hierarchy. Additional CC3 results have been reported in Ref. [38]; those calculations were motivated by the rather large discrepancies to experiment seen at the CCSD level.

The most significant observation with respect to electron correlation is the surprisingly large triples contribution for N_2 and C_2H_2. While the CCS, CC2, and CCSD calculations indicate smooth convergence with the usual reduction in the correlation contributions at each consecutive level and, thus, predict that triple excitation contributions should be rather small, the opposite is seen in the actual calculations [38]. The effect due to triple excitations as obtained at the CC3 level was found to increase the CCSD results by 4% and 16%. Apparently there seems to be no guarantee that triple excitation effects are small when the CC2 model is a good approximation to CCSD. On the other hand, triple excitation effects are found to be rather small for CH_4 (only 1.5% of the CCSD results) [38] consistent with the prediction based on the corresponding CCSD-CC2 difference [74].

Comparison with experiment: MOA. Verdet constants for H_2, N_2, C_2H_2, and CH_4 have been measured at various frequencies (at 1 atm and 298 K) by Ingersoll and Liebenberg [151] in 1956 and are considered to be accurate within

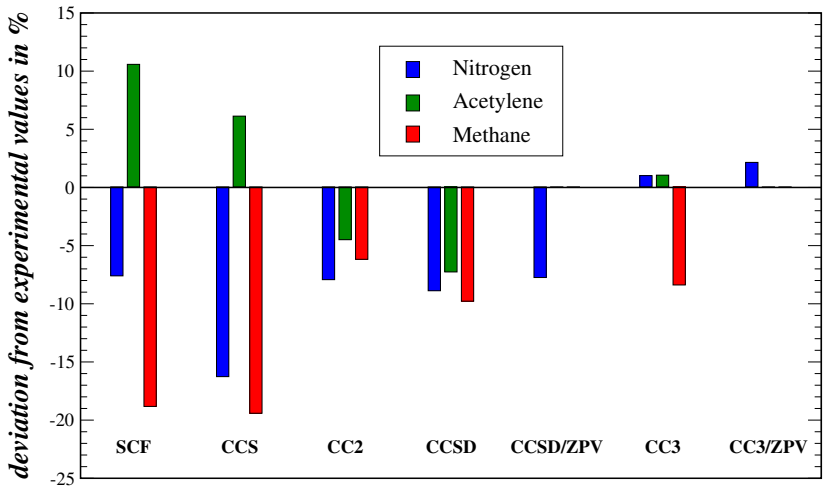


Figure 1.3. Deviation (in percent) from experiment [151] for the calculated Verdet constant $V(\omega)$ of N_2, C_2H_2, and CH_4. The calculations have been carried out in the aug-cc-pVQZ (N_2) and d-aug-cc-pVTZ (C_2H_2 and CH_4) basis sets and at frequency $\omega = 0.11391$ a.u. ZPV corrections for N_2 amount to about 1.3 % and have been determined at the CCSD level (for details see text and Ref. [38]).

1 %. The claimed accuracy has been confirmed in the case of H_2 — by the explicitly correlated results of Bishop and Cybulski [150] and again by the FCI/d-aug-cc-pV5Z results of Ref. [74] (see Table 1.10).

For N_2, C_2H_2, and CH_4, Fig. 1.3 shows the deviation (in percent) from experiment for the calculated Verdet constants. As already discussed, for both N_2 and C_2H_2 triples corrections are substantial, as their inclusion brings the computational results within 1% of the experimental values. However, in the case of N_2 consideration of vibrational effects (about 1.3 %, obtained at the CCSD/t-aug-cc-pVTZ level using a CCSD(T)/aug-cc-pVQZ potential curve [38]) slightly worsens the agreement with experiment, although the result remains within three times the experimental uncertainty (i.e., the 99.9 % confidence interval of the experiment). Whereas the agreement between experimental and calculated Verdet constants can be considered satisfactorily for N_2 and C_2H_2, the situation is quite different for CH_4. The CC3 results for $V(\omega)$ are still about 8-9% lower than the corresponding experimental values (see Fig. 1.3) and, thus, are clearly outside three times the experimental uncertainty. A possible reason for this discrepancy might be the large magnitude of the ZPV effects, whose consideration has been proven important earlier for other properties of methane [114, 152–154]. ZPV correction have been estimated for CH_4 by performing calculations (at the HF-SCF level) for both the equilibrium bond distance (R_e = 1.0858 Å) [155] and the vibrationally averaged bond distance

Table 1.11. CCSD results for the total Verdet constant at $\omega = 0.11391$ a.u. in the case of hydrogen fluoride. Results labeled as "Unrelaxed" refer to the use of the unrelaxed (one-electron) magnetic dipole moment operator together with the usual magnetic-field independent basis sets. Results labeled "Relaxed" include additional contributions due to orbital relaxation in the presence of the magnetic field. Results labeled "LAO" are those obtained when using GIAOs/LAOs.[a]

	Gauge[b]	$V(\omega) \times 10^8$ a.u.		
Basis	origin	Unrelaxed	Relaxed	LAO
cc-pVDZ	CM	1.3365	1.3313	1.2259
	H	0.8713	0.8822	1.2259
aug-cc-pVDZ	CM	2.6116	2.6070	3.0381
	H	2.4365	2.4561	3.0381
aug-cc-pVTZ	CM	2.7843	2.7805	3.0883
	H	2.6473	2.6699	3.0883
d-aug-cc-pVDZ	CM	3.2737	3.2697	3.3473
	H	3.3233	3.2504	3.3473
d-aug-cc-pVTZ	CM	3.2190	3.2153	3.2126
	H	3.1936	3.2186	3.2126

[a] All results taken from Ref. [71]. [b] CM indicates the center of mass.

R_0 = 1.09397 Å [156]. The values obtained for the latter geometry are, for all considered frequencies, by about 2.8% larger than the corresponding equilibrium results, thus indicating the importance of ZPV averaging in the case of CH_4.

Gauge issues: MOA and MCD. Both the Verdet constant $V(\omega)$ of MOR and the B term of MCD suffer from gauge-origin dependence when computed for non-centrosymmetric molecules using approximate quantum chemical models. The gauge-origin dependence can be dealt with for these properties by using GIAOs/LAOs and recasting both quantities in the form of derivatives of a property with respect to an external magnetic field [70,71]. The Verdet constant can be written as a total derivative of the frequency-dependent dipole polarizability with respect to the strength of an external magnetic field:

$$V(\omega) \propto \omega \varepsilon_{\alpha\beta\gamma} \Im\Big(\frac{d\alpha_{\alpha\beta}(-\omega;\omega)}{dB_\gamma}\Big)_0 \tag{1.23}$$

and the B term can be reformulated as the corresponding derivative of the one-photon dipole transition strength $S^{aj}_{\alpha\beta}$:

$$B(a \rightarrow j) \propto \varepsilon_{\alpha\beta\gamma}\left(\frac{d\Im(\langle a|\mu_\alpha|j\rangle\langle j|\mu_\beta|a\rangle)}{dB_\gamma}\right)_0 = \varepsilon_{\alpha\beta\gamma}\Im\left(\frac{dS^{aj}_{\alpha\beta}}{dB_\gamma}\right)_0 . \tag{1.24}$$

Table 1.12. Effect of a gauge-origin shift on the B term for the five lowest dipole-allowed (singlet) transitions from the ground state $X\,A_1$ of formaldehyde (CH_2O) obtained at the CCSD/aug-cc-pVTZ level. The molecule is placed on the xz-plane with the C_2 axis along z and the center of mass (CM) as origin of the coordinate system. Direction of transition in parentheses and excitation energies in atomic units (from Ref. [70]).

Sym.	exc. energy	trans. strength	Gauge origin at CM		Gauge origin at $z = 25$ bohr	
			Unrelaxed	LAO	Unrelaxed	LAO
B_1	0.2659	0.0189 (x)	−1.6844	−1.6819	−1.6325	−1.6819
B_1	0.2987	0.0394 (x)	−31.796	−34.190	−29.899	−34.190
A_1	0.3019	0.0543 (z)	30.776	33.939	32.865	33.939
B_2	0.3433	0.0006 (y)	−0.4109	−0.3640	−0.6172	−0.3640
A_1	0.3578	0.1360 (z)	−10.730	−12.323	−3.3815	−12.323

However, the equivalence of the response functions to the property derivatives is in approximate methods not always strict, as, for example, CC response functions as defined in Sec. 1 do not involve contributions due to orbital relaxation while property derivatives usually do. The incorporation of orbital relaxation effects in the property derivatives is mandatory when perturbation-dependent basis functions such as GIAOs/LAOs are used. Applying the above reformulation to the expressions for $\alpha(-\omega,\omega)$ and S^{aj} obtained from the CC response functions takes only relaxation with respect to the (static) external magnetic field into account [70, 71]. The frequency-dependent electric fields are treated in an unrelaxed manner, which avoids spurious poles due to orbital relaxation (see Sec. 1.2).

The advantage of using GIAOs/LAOs is nicely demonstrated in the case of hydrogen fluoride and formaldehyde (CH_2O). In Table 1.11, results for the Verdet constants $V(\omega)$ of HF are summarized. While those obtained without using GIAOs/LAOs exhibit a distinct gauge-origin dependence (which however becomes smaller for the larger basis sets) gauge-origin independence is preserved in the GIAO/LAO calculations. In addition, it would appear that the use of GIAOs/LAOs leads to a faster basis set convergence as well-known for the calculation of other magnetic properties [157].

Table 1.12 collects first CCSD results for the various contributions to the B term due to the five lowest dipole-allowed electronic transitions in formaldehyde. The lacking gauge-origin independence is here illustrated via calculations for two different gauge origins. Again, the use of GIAOs/LAOs resolves this problem and is thus generally recommended.

4.2 Buckingham effect

For closed-shell systems, the temperature dependence of the BE is given by [40, 134, 135, 158, 159]

$$\Delta n = A_0 + \frac{A_1}{T} \tag{1.25}$$

with $\Delta n = n_{\parallel} - n_{\perp}$ as the corresponding anisotropy of the refractive index,

$$A_0 \propto b(\omega) = \frac{1}{15}\{B_{\alpha\beta,\alpha\beta} - \mathcal{B}_{\alpha,\alpha\beta,\beta}\} - \frac{5}{\omega}\varepsilon_{\alpha\beta\gamma}J'_{\alpha,\beta,\gamma} \tag{1.26}$$

$$A_1 \propto -\Theta_{\alpha\beta}\alpha_{\alpha\beta} - \mu_\alpha\left(A_{\beta,\alpha\beta} + \frac{5}{\omega}\varepsilon_{\alpha\beta\gamma}G'_{\beta,\gamma}\right) \tag{1.27}$$

and

$$B_{\alpha\beta,\gamma\delta}(-\omega;\omega,0) \propto \Re\langle\langle\hat{\mu}_\alpha;\hat{\mu}_\beta,\hat{\Theta}_{\gamma\delta}\rangle\rangle_{\omega,0} \tag{1.28}$$

$$\mathcal{B}_{\alpha,\beta\gamma,\delta}(-\omega;\omega,0) \propto \Re\langle\langle\hat{\mu}_\alpha;\hat{\mu}_\delta,\hat{\Theta}_{\beta\gamma}\rangle\rangle_{0,\omega} \tag{1.29}$$

$$J'_{\alpha,\beta,\gamma}(-\omega;\omega,0) \propto \Im\langle\langle\hat{\mu}_\alpha;\hat{m}_\beta,\hat{\mu}_\gamma\rangle\rangle_{\omega,0} \tag{1.30}$$

$$\alpha_{\alpha\beta}(-\omega;\omega) \propto \Re\langle\langle\hat{\mu}_\alpha;\hat{\mu}_\beta\rangle\rangle_{\omega} \tag{1.31}$$

$$A_{\alpha,\beta\gamma}(-\omega;\omega) \propto \Re\langle\langle\hat{\mu}_\alpha;\hat{\Theta}_{\beta\gamma}\rangle\rangle_{\omega} \tag{1.32}$$

$$G'_{\alpha,\beta}(-\omega;\omega) \propto \Im\langle\langle\hat{\mu}_\alpha;\hat{m}_\beta\rangle\rangle_{\omega}. \tag{1.33}$$

In the equations above, μ and Θ indicate the permanent dipole and (traceless) quadrupole moments, respectively. In the case of non-dipolar molecules the birefringence becomes

$$\Delta n \propto b(\omega) + \frac{2\Theta_{\alpha\beta}\alpha_{\alpha\beta}}{15kT} = b(\omega) + \frac{F}{T}\,, \tag{1.34}$$

and for spherical systems it reduces to [159, 160]

$$\Delta n \propto b(\omega)\,. \tag{1.35}$$

The connection between BE and MOA are evident, as the response function in Eq. (1.30) also appears in the corresponding expression for the Verdet constant $V(\omega)$, Eq. (1.21), though with a different frequency argument. The response function in Eq. (1.30) plays also a central role in the BE, as for low frequencies it constitutes the most important contribution to the temperature-independent term $b(\omega)$ and as it is solely responsible for the BE in the case of spherical systems. A more detailed discussion concerning the relationship between $V(\omega)$ and $b(\omega)$ can be found in Refs. [160] and [149].

Basis set convergence. The basis set convergence in the quantum chemical calculation of the temperature-independent contribution to the BE has been investigated for several different small molecules in Ref. [149, 161–164]. Due to the different operators involved in the response functions required for the calculation of $b(\omega)$, it is difficult to put forward theoretical arguments or simple rules concerning the basis set convergence. Nevertheless, smooth convergence with extension of basis set is observed in all cases investigated so far. To some extent this is probably due to some error cancellation as the involved quadrupole hyperpolarizabilities are usually known to be quite demanding with respect to the size of basis sets.

Overall, it seems that—similar to the calculation of hyperpolarizabilities—(doubly) augmented basis sets of at least triple-ζ or better quadruple-ζ quality are required to obtain reasonable results, as the use of non-augmented basis sets might even lead to qualitatively wrong results, i.e., a wrong sign of $b(\omega)$. For N_2 monotonic convergence is observed for both the singly augmented and the doubly augmented series and the two series approach the basis set limit from different sides [161]. The good convergence achieved in such calculations is, for example, seen by the fact that for X = Q the remaining differences are with 0.2 % rather small. Similar trends are also seen for the other molecules [161, 162], although the convergence pattern is for Cl_2 somewhat less regular [163].

Convergence with correlation treatment. The temperature-independent contribution $b(\omega)$ as well as the other BE related terms have so far mostly been computed either at HF-SCF and/or CCSD levels. For Ne and Ar CCS and CC2 results have also been reported [149]. CO is the only case for which CC3 results are available [165]. Overall, it is seen that correlation effects are not negligible and in some cases even larger than the remaining basis set effects. For example, they amount (based on CCSD results) to about 0.5% for N_2, 15% for acetylene, and 11% for methane [161]. In the case of CO inclusion of triple excitation effects (at the CC3 level) lead to a substantial decrease (about 8 to 10%) in $b(\omega)$ in comparison to the CCSD results. Their inclusion thus seems to be essential when aiming at a rigorous comparison with experiment.

Comparison with experiment: Quadrupolar molecules. The experimental importance of the BE is due to the fact that it allows the experimental determination of molecular electric quadrupole moments Θ. The procedure is based on Eq. (1.34) and was first proposed by Buckingham [134] in the late fifties. With the assumption that the molecular polarizability is known, Θ can be extracted from measurements of Δn. In order to separate the A_0 from the A_1 contribution, it is necessary to perform BE measurements over an appropriately large temperature range.

Nevertheless, in several cases measurements were carried out only at a single temperature and the contribution due to A_0 was assumed to be much smaller than F/T and consequently neglected. Quadrupole moments obtained in this way are referred to as "apparent" quadrupole moments and are not necessarily identical to the actual quadrupole moment of the molecule.

In other cases [166, 167] literature values for (supposedly) $b(\omega)$ taken from quantum chemical calculations were used to separate the A_0 and A_1 contributions. While this is in principle preferred over the first approach, the use of computational data leads to questions concerning their reliability, as low-level data might easily deteriorate the accuracy of the quadrupole moments obtained in this way. In addition, there has been some confusion in the earlier literature concerning the hyperpolarizability correction term $b(\omega)$. In the original papers by Buckingham and coworkers [134, 168] this term was called B and was referred to as a quadrupole hyperpolarizability. This was apparently misunderstood and led to the incorrect use of the averaged static dipole-dipole-quadrupole hyperpolarizability $\frac{2}{15}B_{\alpha\beta\alpha\beta}$ as correction term instead of $b(\omega)$ in the determination of the quadrupole moment [166, 167].

The most striking example of the consequences of these different assumptions and choices is the N_2 case. In 1998 Graham and co-workers [167] published an experimental result for the quadrupole moment of N_2 based on a single temperature measurement of the birefringence. The measured apparent quadrupole moment (obtained by neglecting the A_0 term) was found to be $(-5.25\pm0.08)\times10^{-40}$ Cm^2. After revision with an incorrect A_0 value taken from the literature, the quadrupole moment of N_2 was determined to $(-4.65\pm0.08)\times10^{-40}$ Cm^2, i.e., noticeably lower than previous experimental and theoretical estimates.

Using our CCSD results [161] for $b(\omega)$, we redetermined the experimental moment from the birefringence measurement of Graham and coworkers to $(-5.01 \pm 0.08) \times 10^{-40}$ Cm^2—now in excellent agreement with the best currently available theoretical results ($(-4.93 \pm 0.03) \times 10^{-40}$ Cm^2 [169], see Table 1.13).

More recently, Ritchie, Watson and Keir [170] carried out new experiments on the BE of N_2 for a variety of different temperatures, thus enabling a proper separation of the temperature-independent contribution from the orientational term. These authors also performed new measurements for the polarizability anisotropy. Combining all their experimental data, they were able to extract a new experimental value of $(-4.97 \pm 0.16) \times 10^{-40}$ Cm^2 for the quadrupole moment of N_2. The good agreement with the previous (with the CCSD result) revised experimental value as well as the corresponding theoretical results (see Table 1.13) clearly eliminates any remaining doubts concerning the experimental quadrupole moment of N_2.

Table 1.13. Theoretical estimates and experimental values for the quadrupole moment Θ, the orientational term F/T, and temperature independent correction $b(\omega)$ (all quantities in atomic units and for T=273.15K) for N_2, C_2H_2, Cl_2, CO_2, and CS_2.

	Θ		F/T	$b(\omega)$	
	Theory	Exp.	Theory	Theory	Exp.
N_2	-1.098 ± 0.007[a]	-1.11 ± 0.04[b]	-785.1[c]	-36.13[c]	-76.62 ± 23.57[b]
		-1.12 ± 0.02[d]			
C_2H_2	4.79 ± 0.03[e]	4.66 ± 0.19[f]	9257[c]	-193.3[c]	
Cl_2	2.327 ± 0.010[g]	$2.31/2.36\pm0.04$[h]	-6479.9[i]	-213.6[i]	
CO_2	-3.185 ± 0.020[j]	-3.187 ± 0.13[k]	-7536.7[l]	-54.46[l]	-159 ± 77[k]
		-3.18 ± 0.14[m]			-118 ± 178[n]
CS_2	2.338[o]	2.56 ± 0.11[k]	25500[p]	-410[p]	-1179 ± 766[k]

[a] Ref. [169]. CCSD(T) basis set limit including ZPV corrections, estimates of correlation beyond CCSD(T), and relativistic effects. [b] Ref. [170]. [c] Ref. [161]. CCSD/d-aug-cc-pVQZ/frozen-core equilibrium results. [d] the apparent moment Θ^{eff}=-1.170 in Ref. [167] after revision with b from Ref. [161]. [e] Ref. [171]. ZPV corrected CCSD(T) basis set limit including estimates for correlation beyond CCSD(T) and relativistic effects. [f] the apparent moment Θ^{eff}=-4.55 ± 0.22 in Ref. [173] after revision with b from Ref. [161]. [g] Ref. [163]. ZPV corrected CCSD(T) basis set limit including estimates for correlation beyond CCSD(T) and relativistic contributions. [h] Ref. [163]. Revision of the apparent quadrupole moment (2.23 ± 0.04) in [167] with the calculated $b(\omega)$. [i] Ref. [163]. ZPV corrected CCSD/d-aug-cc-pVQZ result including relativistic and pure vibrational corrections. [j] Ref. [162]. ZPV corrected CCSD(T) basis set limit including estimates for correlation beyond CCSD(T) and relativistic effects. [k] Ref. [172]. [l] Ref. [162]. CCSD/d-aug-cc-pVQZ/frozen-core equilibrium results. [m] Ref. [167]. [n] Ref. [174]. [o] Ref. [162]. CCSD(T)/d-aug-cc-pVQZ/frozen-core equilibrium value. [p] Ref. [162]. CCSD/aug-cc-pVQZ/frozen-core equilibrium value.

Revisions of the apparent quadrupole moments of quadrupolar systems based on *ab initio* results for $b(\omega)$ were undertaken in the last few years for Cl_2 [163] and C_2H_2 [161, 171] (see Table 1.13)). Direct comparison of the hyperpolarizability terms $b(\omega)$ calculated *ab initio* and derived from measurements at various temperatures, such as in the case of CO_2, CS_2 [172] and the most recent results for N_2 [170] turns out to be difficult in all cases due to the very large error bars associated with the experimentally derived results (see Table 1.13).

Comparison with experiment: Atoms and spherical systems. From a theoretical point of view, rare gas atoms are ideal test systems. This is also the case for the BE, as for these systems the BE is entirely due to the hyperpolarizability term $b(\omega)$. Table 1.14 collects our "best theoretical results" for the hyperpolarizability term $b(\omega)$ of all atomic and spherical systems investigated so far together with the available experimental data in the literature.

From the data in Table 1.14, it is possible to derive estimates for the anisotropy Δn under some hypothetical standard experimental conditions for pressure,

Table 1.14. Best theoretical estimates and experimental values of the hyperpolarizability contribution $b(\omega)$ at 632.8 nm (in atomic units).

System	Theory	Experiment
Helium	-3.15[a]	
Neon	-5.89[b]	
Argon	-58.0[c]	0 ± 109[d]
Krypton	-117.90[e]	
CH_4	-97.3[f]	-262 ± 66[d]
SF_6	-95[g]	0 ± 109[d]

[a] Ref. [149]. FCI/d-aug-cc-pV6Z results. [b] Ref. [149]. CCSD/d-aug-cc-pV5Z results. [d] Ref. [176]. [e] Ref. [40]. CCSD/d-aug-cc-pV5Z results. [f] Ref. [161]. CCSD/d-aug-cc-pVQZ results. [g] Ref. [149]. CCSD/d-aug-cc-pVDZ results.

temperature, path length and electric field gradient, see Refs. [40,70,159]. For both helium and neon, it appears that the BE is too small to be detected with current experimental devices (for a discussion, see Ref. [175]). For krypton, CH_4, and SF_6 theory predicts birefringences of approximatively the same size and about twice as large as for argon. Experimentally, it has so far not been possible to detect the BE for argon and SF_6 [176]. For CH_4 theory and experiment agree on the sign of the effect, but the theoretical value is much smaller, although still within three standard deviations of the experiment. Clearly the computational results need to be improved and (as already discussed for the Verdet constant of methane) ZPV effects need to be considered before a final judgment of the experimental value seems appropriate. To our knowledge, no experimental data is available for krypton.

Comparison with experiment: Dipolar species. Experimental measurements of the BE can also be used to determine quadrupole moments for dipolar systems. The values obtained in this way refer to an origin which is denoted as the effective quadrupole center (EQC) [135]. The EQC is defined as the point at which the combination of dipole-quadrupole and dipole-magnetic dipole polarizabilities multiplied with the dipole moment given in Eq. (1.27) vanishes so that an expression for the BE similar to the one for quadrupolar molecules, Eq. (1.34), is recovered.

The position of the effective quadrupole center, R_z, cannot be determined from the BE experiment and has to be identified by means of calculations. This is usually done by determining the origin shift which is necessary to makes the dipolar contribution in the A_1 term to zero.

Two semiclassical theories existed in the literature for the BE of dipolar species, one due to Buckingham and coworkers (BLH) [134,135,160], and one due to Imrie and Raab (IR) [158]. In Refs. [159, 162–165], it was shown by

Table 1.15. Computed and experimentally derived effective quadrupole centers (EQC, R_z, in bohr) with respect to the center of mass for CO at 632.8 nm. The molecule is oriented along the z axis with positive direction pointing from C to O, so that the dipole moment is positive. CCSD/d-aug-cc-pVQZ results are from Ref. [164]. CC3/d-aug-cc-pVQZ results are from Ref. [165]. The computed shifts are ro-vibrationally corrected.

Property	BLH	IR
R_z^{CCSD}	4.52±0.5	2.50±0.5
R_z^{CC3}	5.96±0.5	3.06±0.5
$R_z^{\mathrm{exp,app}}$ [a]	7.7±0.5	
$R_z^{\mathrm{exp,CCSD}}$ [b]	6.25±0.51	5.78±0.51
$R_z^{\mathrm{exp,CC3}}$ [c]	6.16±0.51	5.69±0.51

[a] "Apparent" experimentally derived shift obtained from $\Theta^{(R_z)} = \Theta^{(CM)} - 2R_z\mu$ combining the experimental values for the dipole moment μ, the apparent quadrupole moment Θ^{eff} from Buckingham birefringence and the quadrupole moment at the center of mass Θ^{CM} from molecular beam electric resonance. [b] The experimentally derived value where Θ^{eff} from Buckingham birefringence has been corrected for $b(\omega)$ computed at the CCSD level. See Refs. [164,165] for details. [c] The experimentally derived value where Θ^{eff} from Buckingham birefringence has been corrected for $b(\omega)$ computed at the CC3 level. See Refs. [164,165] for details.

means of quantum chemical calculations that these two theories led to different numerical results for the induced anisotropy in a variety of cases. The differences could not be ascribed to deficiencies in the computational approach, as they persisted even for two-electron systems (such as helium and H_2 [159]), for which practically "exact" results are available.

The most striking disagreement was observed for the EQC and the resulting quadrupole moment of CO [164,165]. In our first study [164] CCSD(T) calculations for the quadrupole moment at the center of mass and CCSD calculations for the EQC were used to determine the quadrupole moment with respect to the EQC within both theories. Our results slightly favored the BLH theory, but the computations were not of sufficient accuracy to decide unambiguously which of the two theories could be correct.

In Ref. [165], a second analysis was carried out focusing on the remaining deficiencies in the used computational approach. The main aspect was that the EQCs were now determined using the CC3 approach with an inclusion of triple excitations. The obtained results for the EQC are summarized in Table 1.15.

The CC3 data clearly favored the BLH theory, but did not supply any explanation for the discrepancy between the two theories. Triggered by these results, a revision of both theories has been recently undertaken and an error in the IR approach was identified and corrected (for details, see Ref. [177,178]).

4.3 Cotton–Mouton effect

The general expression of CME [136,137] has for diamagnetic fluids the form of Eq. (1.25), where now A_0 and A_1 involve the following properties [179,180]

$$A_0 \propto \Delta\eta(\omega) = \frac{1}{5}\Big(\eta_{\alpha\beta,\alpha\beta} - \frac{1}{3}\eta_{\alpha\alpha,\beta\beta}\Big) \tag{1.36}$$

$$A_1 \propto \Big(\alpha_{\alpha\beta}\xi_{\alpha\beta} - \frac{1}{3}\alpha_{\alpha\alpha}\xi_{\beta\beta}\Big) \tag{1.37}$$

$\xi_{\alpha\beta}$ is the magnetizability and $\eta_{\alpha\beta,\gamma\delta}$ the hypermagnetizability tensor

$$\eta_{\alpha\beta,\gamma\delta} = \eta^{dia}_{\alpha\beta,\gamma\delta}(-\omega;\omega,0) + \eta^{para}_{\alpha\beta,\gamma\delta}(-\omega;\omega,0,0) \tag{1.38}$$

$$\eta^{para}_{\alpha\beta,\gamma\delta}(-\omega;\omega,0,0) \propto \Re\langle\langle\hat{\mu}_\alpha;\hat{\mu}_\beta,\hat{m}_\gamma,\hat{m}_\delta\rangle\rangle_{\omega,0,0} \tag{1.39}$$

$$\eta^{dia}_{\alpha\beta,\gamma\delta}(-\omega;\omega,0) \propto \Re\langle\langle\hat{\mu}_\alpha;\hat{\mu}_\beta,\hat{\xi}^{dia}_{\gamma\delta}\rangle\rangle_{\omega,0} \tag{1.40}$$

where $\hat{\xi}^{dia}$ is the diamagnetic susceptibility operator, and the other quantities were already defined above. As for BE above, the inverse-temperature contribution dies out for spherical systems, where thus the anisotropy is entirely given by the higher order contribution A_0

$$\Delta n \propto \Delta\eta(\omega) \tag{1.41}$$

Convergence with the basis set. Table 1.16 shows the results of a basis set study from Ref. [39] for the anisotropy of the hypermagnetizability $\Delta\eta$ and the all–parallel component $\eta_{zz,zz}$ at the CC3 level for Ne and Ar. As it can be inferred from the table, the convergence of η with the increase in the cardinal number X and the augmentation level n of the n-aug-cc-pVXZ series is mostly monotonic and smooth, especially for neon. Similar to the purely electric second hyperpolarizability $\gamma_{||}$, the results converge very slowly with the singly-augmented basis sets and triply augmentation is needed for atoms to obtain good convergence with the cardinal number. As for $\gamma_{||}$, at least triple-ζ basis sets are required to obtain a qualitatively correct description. With the t-aug-cc-pVQZ and t-aug-cc-pV5Z basis sets the results are expected to be converged is within a few percent, both for the individual components and for the anisotropy. When core–valence basis sets are employed in all–electron calculations the differences are for Ne in the order of 0.03 a.u. or $\approx 1\%$ for X = T, dropping to ≈ 0.01 a.u. or $\approx 0.3\%$ for X = Q. For argon the effect of the core functions is somewhat larger, in particular for the anisotropy $\Delta\eta$.

Convergence with electron correlation treatment. The need for an accurate account of electron correlation for the high-order properties involved in

Table 1.16. Cotton-Mouton effect in neon and argon. CC3 response results for the static limit (from Ref. [39], all–electron calculations, results in a.u.).

Basis Set	Neon		Argon	
	$\eta_{zz,zz}$	$\Delta\eta$	$\eta_{zz,zz}$	$\Delta\eta$
aug-cc-pVDZ	−1.61	0.50	−16.8	5.2
aug-cc-pVTZ	−2.13	0.96	−20.8	11.7
aug-cc-pVQZ	−2.60	1.47	−24.0	17.3
aug-cc-pV5Z	−2.87	2.04	−21.7	19.9
d-aug-cc-pVDZ	−3.67	1.60	−32.3	13.6
d-aug-cc-pVTZ	−3.38	2.21	−24.1	22.6
d-aug-cc-pVQZ	−3.15	2.54	−22.7	23.5
d-aug-cc-pV5Z	−2.96	2.86	−21.7	24.6
t-aug-cc-pVDZ	−3.92	1.72	−32.1	13.5
t-aug-cc-pVTZ	−3.07	2.83	−22.3	25.5
t-aug-cc-pVQZ	−2.94	2.87	−21.6	25.1
t-aug-cc-pV5Z	−2.93	2.91		
t-aug-cc-pCVTZ	−3.05	2.82	−22.1	25.1
t-aug-cc-pCVQZ	−2.94	2.87	−21.5	24.8

CME, JB and MEB is particularly evident in systems of spherical symmetry, where these properties provide the whole contribution to the observable.

Table 1.17 summarizes the results of a benchmark study for the convergence of $\Delta\eta$ for neon with the correlation treatment in a series of CC methods from Ref. [39]. Whereas CCSD yields results still ca. 3% too low (orbital-relaxed) or 1.4% too high (orbital-unrelaxed), the CCSDT results differs from the FCI limit by only 0.002 a.u. or $\approx 0.1\%$. Thus CCSDT provides for the Cotton–Mouton effect of Ne results which are converged within approximately 0.1%.

Figure 1.4 shows the convergence behavior of the (static) hypermagnetizability anisotropy $\Delta\eta(0)$ of neon and argon up to CCSDT in the fairly large basis sets d-aug-cc-pV5Z (Ne) and d-aug-cc-pVQZ (Ar). The orbital-relaxed results were obtained for HF-SCF, MP2, CCSD, CCSD(T), CC3 and CCSDT by numerical differentiation of analytically computed magnetizabilities. A second

Table 1.17. Convergence of the anisotropy of the static hypermagnetizability $\Delta\eta(0)$ of neon with the correlation treatment (from Ref. [39]; finite field orbital–relaxed results (unless specified) for d-aug-cc-pVDZ, frozen core approximation for $1s$ shell, numbers in atomic units.).

CCSD	CCSD (unrel.)	CCSDT	CCSDTQ	CCSDTQP	FCI
1.546	1.614	1.594	1.593	1.593	1.592

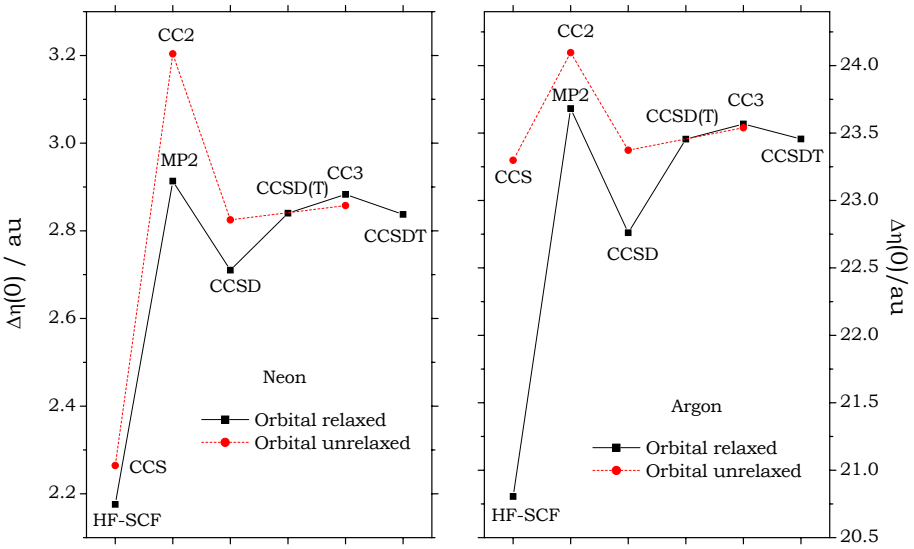


Figure 1.4. Static hypermagnetizability anisotropy, $\Delta\eta(0)$, computed with the d-aug-cc-pV5Z basis set (Neon) and d-aug-cc-pVQZ basis set (Argon). Orbital-relaxed results obtained with a finite field approach from analytically evaluated magnetizabilities are compared to those obtained from orbital-unrelaxed quadratic and cubic response functions.

series of orbital-unrelaxed results was obtained via analytic quadratic and cubic response functions for the CCS, CC2, CCSD and CC3 wavefunction models. Figure 1.4 illustrates how the two series converge to a common limit as the level of electron correlation is increased. For instance for neon, the CCSD results obtained in the two approaches differ by almost 10%, while at the CC3 level the difference is five times smaller. These percentages are sensibly smaller for argon. It is expected that at the CCSDT level the orbital-relaxed and unrelaxed approaches give essentially the same results. In the orbital-relaxed hierarchy the contribution of connected triples (CCSDT vs. CCSD) increases the anisotropy by $\approx$ 3–5 %. In the unrelaxed hierarchy the triples effect seems to be somewhat smaller. The latter hierarchy was used to calculate the CME at the experimental wavelength.

Comparison with experiment. Table 1.18, taken from Ref. [39] (see also Ref. [40]), shows a comparison between theory and experiment for the CME of neon and argon gas. For the best non-relativistic theoretical results the absolute uncertainties can be placed around 0.1 a.u. for Ne and (probably) around 1 a.u. for Ar, i.e. in the order of 2–3%. They substantiate the claim that, at least in this case, the computational results should be considered the

Table 1.18. Comparison of experimental and computational results for the hypermagnetizability anisotropy $\Delta\eta(\omega)$ of neon and argon. Atomic units.

	λ	Theory	Experiment
Neon	∞	2.89(10)[a,b]	
	790 nm		3.2±1.2[c]
	514.5 nm		1.4±0.1[d]
Argon	∞	24.7[b]	
	790 nm		27±5[c]
	514.5 nm		30.0±4.5[e]

[a] The number in parenthesis indicates the estimated absolute error on the last digit. [b] Ref. [39]. Static value estimated at CCSDT level; frequency dependence estimated using CC3 analytic response (and found to be negligible). [c] Ref. [181], pressure of 1.52×10^5 Pa, temperatures in the range 285-293 K. The value is estimated for an average of 289 K. [d] Ref. [182], temperature of 298.15 K and extrapolated at a pressure of 1 atm. [e] Ref. [183].

reference nowadays. For instance the hypermagnetizability of argon is of a magnitude that allows a relatively easy measurement and can be computed with an accuracy more than one order of magnitude better than presently afforded by experiment. Thus, currently it appears advantageous to use the computed value for argon as a standard for calibration of the optical apparata employed for CME measurements.

4.4 Jones and magnetoelectric birefringence

As for BE and CME, also for JB and MEB the birefringence can be expressed with a general relationship such as Eq. (1.25). In this case it is [141, 143, 184]:

$$\begin{aligned} A_0 \;\propto\; & 3G_{\alpha,\beta\alpha\,\beta} + 3G_{\alpha,\beta\beta,\alpha} - 2G_{\alpha,\alpha\beta,\beta} \\ & -\frac{\omega}{2}\varepsilon_{\alpha\beta\gamma}(a'_{\alpha,\beta\delta,\delta,\gamma} + a'_{\alpha,\beta\delta,\gamma,\delta}) \qquad (1.42) \\ A_1 \;\propto\; & \mu_\alpha(3G_{\alpha,\beta\beta} + 3G_{\beta,\alpha\beta} - 2G_{\beta,\beta\alpha}) \\ & -\frac{\omega}{2}\varepsilon_{\alpha\beta\gamma}(\mu_\gamma a'_{\alpha,\beta\delta,\delta} + \mu_\delta a'_{\alpha,\beta\delta,\gamma}) \qquad (1.43) \end{aligned}$$

and now

$$\begin{aligned} a'_{\alpha,\beta\gamma,\delta,\epsilon}(-\omega;\omega,0,0) &\propto \Im\langle\langle\hat{\mu}_\alpha;\hat{q}_{\beta\gamma},\hat{m}_\delta,\hat{\mu}_\epsilon\rangle\rangle_{\omega,0,0} && (1.44)\\ G_{\alpha,\beta\gamma,\delta}(\omega) &= G^{para}_{\alpha,\beta\gamma,\delta}(\omega) + G^{dia}_{\alpha,\beta\gamma,\delta}(\omega) && (1.45)\\ G^{para}_{\alpha,\beta\gamma,\delta}(-\omega;\omega,0,0) &\propto \Re\langle\langle\hat{\mu}_\alpha;\hat{m}_\beta,\hat{m}_\gamma,\hat{\mu}_\delta\rangle\rangle_{\omega,0,0} && (1.46)\\ G^{dia}_{\alpha,\beta\gamma,\delta}(-\omega;\omega,0) &\propto \Re\langle\langle\hat{\mu}_\alpha;\hat{\xi}^{dia}_{\beta\gamma},\hat{\mu}_\delta\rangle\rangle_{\omega,0} && (1.47)\\ a'_{\alpha,\beta\gamma,\delta}(-\omega;\omega,0) &\propto \Im\langle\langle\hat{\mu}_\alpha;\hat{q}_{\beta\gamma},\hat{m}_\delta\rangle\rangle_{\omega,0} && (1.48) \end{aligned}$$

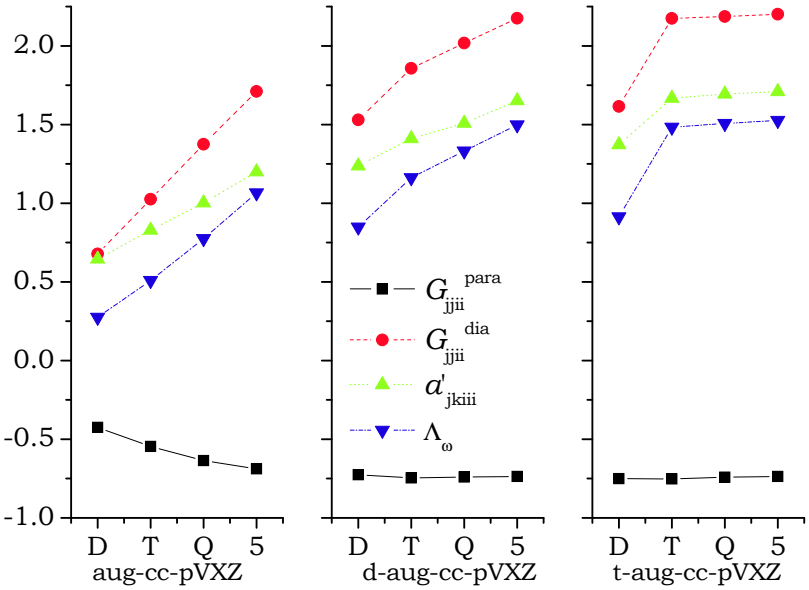


Figure 1.5. Contributions to the Jones and magneto-electric birefringences of neon. CC3 all–electron response results in atomic units.

$$G_{\alpha,\beta\gamma}(\omega) = G^{para}_{\alpha,\beta\gamma}(\omega) + G^{dia}_{\alpha,\beta\gamma}(\omega) \tag{1.49}$$

$$G^{para}_{\alpha,\beta\gamma}(-\omega;\omega,0) \propto \Re\langle\langle\hat{\mu}_\alpha;\hat{m}_\beta,\hat{m}_\gamma\rangle\rangle_{\omega,0} \tag{1.50}$$

$$G^{dia}_{\alpha,\beta\gamma}(-\omega;\omega) \propto \Re\langle\langle\hat{\mu}_\alpha;\hat{\xi}^{dia}_{\beta\gamma}\rangle\rangle_{\omega} \tag{1.51}$$

where $\hat{q}$ is the traced quadrupole moment operator.

Convergence with the basis set. The basis set convergence of the response functions that enter the expressions for JB and MEB are illustrated in Figs. 1.5 and 1.6 with CC3 results for Ne and Ar from Ref. [185]. As demonstrated before in Ref. [184], the non- and singly-augmented basis sets (cc-pVXZ and aug-cc-pVXZ) are inadequate for mixed electric and magnetic field birefringences. An acceptable rate of convergence requires at least doubly-augmented basis sets, but for the atoms Ne and Ar the third set of diffuse functions in the t-aug-cc-pVXZ series still improves the convergence. As for other third- and fourth-order magneto-electric properties double-ζ basis sets give rise to rather large errors, while beyond the DZ level the changes with the cardinal number are smooth. With respect to convergence with the one-electron basis set the most demanding contributions to $\Lambda_\omega = G_{jjii} + \frac{\omega}{2}a'_{jkiii}$—and thus to the observable Δn—are G^{dia} and a', i.e. the quadratic response functions which involve both the electric dipole and quadrupole operators. Similar as for $\gamma_{||}$ and η, at least t-

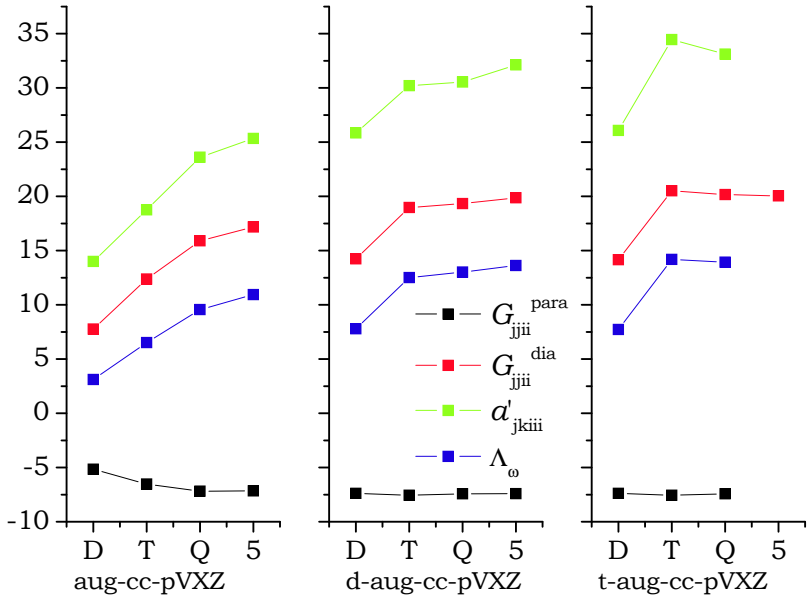


Figure 1.6. Contributions to the Jones and magneto-electric birefringences of argon. CC3 all–electron response results in atomic units.

aug-cc-pVTZ basis sets appear to be needed for atoms to guarantee a good level of confidence that basis set convergence is approached for these contributions. With these basis sets the results seem to be converged within a few percent. (For further information on the basis set convergence for JB and MEB for other atoms and molecules the reader is refereed to Ref. [184].)

Convergence with electron correlation treatment. Figure 1.7 illustrates the convergence of the response properties involved in JB and MEB with the improvement of the electron correlation treatment in the hierarchy HF-SCF, CCS, CC2, CCSD, CC3. The results are those obtained for neon and argon, using the d-aug-cc-pV5Z and d-aug-cc-pVQZ basis sets, respectively, in all electron calculations within an orbital-unrelaxed approach. Again, the convergence is somewhat slower for neon than for argon, with HF-SCF and CCS on one side and CC2 on the other side of CCSD and CC3. After some initial oscillations, all properties seem to be quite well converged at the CCSD level, with CC3 yielding only small corrections. The triples effect on the observable, measured by comparing CCSD and CC3 results, are for Ne and Ar in the order of 1%. In Ref. [185] it is shown that these percentages increase to $\approx$ 2–3% for nitrogen and even higher (ca. 6%) for CO and can in some cases be notably higher for the individual response properties than for the total observable.

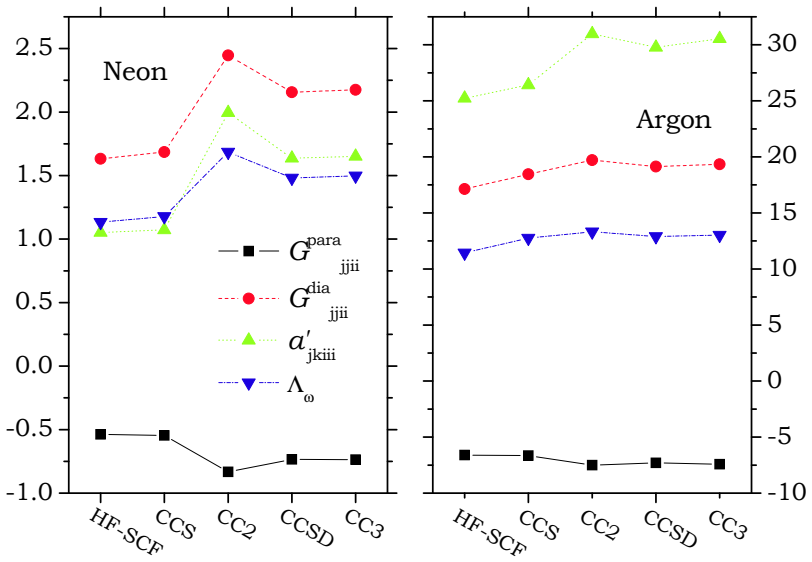


Figure 1.7. JB and MEB of neon and argon. Analytical response result, all electron, unrelaxed orbitals.

Comparison with experiment. Measurements of JB and MEB are a very recent occurrence, and they have been limited so far to systems in the condensed phase [186–188], where measurable birefringences can be observed in optical paths of the order of centimeters. Computational analysis has been limited, on the other hand to the gas phase [40, 184, 185, 189, 190]. However, optical

Table 1.19. Comparison of estimated JB and MEB with the values computed for CME. ϕ is the retardance ($\phi = 2\pi l \Delta n/\lambda$), i.e. the property which is actually measured. λ = 632.8 nm, path length l = 1 m, pressure P = 1 bar, temperature T = 273.15 K, electric field strength E = 2.6 $\times 10^6$ V m^{-1}, magnetic induction field B = 3 T. The acronym nXZ is a shorthand notation for the correlation consistent n-aug-cc-pVXZ basis set. "Wf" is the wave function model employed. From Ref. [40].

	Jones			CME		
	$\Delta n/10^{-15}$	Basis/Wf	ϕ/nrad	$\Delta n/10^{-12}$	Basis/Wf	ϕ/nrad
Ne	−0.035	t5Z/CC3	−0.35	0.00581	t5Z/CCSDT	5.8×10^{1}
Ar	−0.30	t5Z/CC3	−3.0	0.0497	d5Z/CC3	4.9×10^{2}
N_2	−0.75	dQZ/CCSD	−7.4	−2.84	tTZ/B3LYP	-2.8×10^{4}
C_2H_2	−3.0	aQZ/CCSD	−30	−1.50	aTZ/MCSCF	-1.5×10^{4}
CO	−1.2	dQZ/CCSD	−12	−1.80	tTZ/B3LYP	-1.8×10^{4}

apparata designed for measurements in the gas phase of other birefringences, as the Kerr and Cotton-Mouton effects, may in principle be adapted to measure JB and MEB. It is thus probably useful to provide reliable predictions of the magnitude of the effect. Table 1.19 shows a comparison from Ref. [40] of predicted birefringences and corresponding retardances for the two birefringences discussed in this section, i.e. CME and JB (or MEB).

For these systems Jones and magneto-electric birefringences yield retardances which are under the usual experimental conditions about two orders of magnitude weaker than those observed for CME. For the rare gases the predicted retardances for the JB and MEB are comparable to those of BE. The current detection limit for retardances of ≈ 2 nrad [175] makes their observation in these systems rather challenging, but they should be measurable for N_2, CO and even better for C_2H_2.

5. Conclusions and Outlook

The calculation of NLO properties with high accuracy is a very challenging task requiring consideration of many different issues, including the electronic, vibrational, and condensed phase contributions. In this review we have described the application of CC response methods for the calculation of the electronic contributions to first and second hyperpolarizabilities as well as some magneto-optical NLO properties. As a result of many years work on implementing CC response theory [46,47,58–63,65–71,191–203] we can nowadays employ CC methods for detailed and accurate studies of many different molecular properties. A cornerstone has been the CC3 wavefunction model. The development of efficient implementations for these methods has required a significant effort. Yet, actual applications are today still limited to small systems. The pay-back is, however, that high accuracy can indeed be obtained with CC3. Since electron correlation is typically of extreme importance for NLO properties the CC3 model stands central for such calculations. With the accuracy obtained at this level the interpretation of experiments can be discussed with confidence.

Looking into the future for the calculation of NLO properties for small molecules some challenges remain. A basic problem is that the standard CC wavefunction models including CCSD and CC3 are single-reference methods. While for multi-reference cases MCSCF response theory can be applied, for more than a few electrons it will still be very difficult to achieve an accuracy comparable to that obtained in CC calculations on closed–shell single-reference molecules. A more practical restriction in the present implementations of CC3 response theory is that it does not include open–shell molecules even when they can be described by single reference theory. However, very recently an open–

shell CC3 implementation (using one additional approximation) was presented for response calculations of excitations [204].

The example of neon, where relativistic contributions account for as much as $\approx 0.5\%$ of $\gamma_{||}$, shows that relativistic effects can turn out to be larger for high-order NLO properties and need to be included if aiming at high accuracy. Some efforts to implement linear and nonlinear response functions for two- and four-component methods and to account for relativity in response calculations using relativistic direct perturbation theory or the Douglas-Kroll-Hess Hamiltonian have started recently [131, 205, 206]. But presently, only few numerical investigations are available and it is unclear when it will become important to include relativistic effects for the frequency dispersion.

An important issue for magneto-optical properties is gauge origin independence. GIAOs/LAOs are a widely applied approach to ensure gauge origin independence in *ab initio* calculation of properties that involve static magnetic fields. For frequency-dependent magnetic fields it is a still unsolved problem how gauge origin independence can be ensured in approximate calculations. GIAOs include the magnetic field already at the level of basis functions and thus necessarily in the uncorrelated reference function. This is incompatible with the requirement that the frequency-dependence of the wavefunction should solely be determined through a single–step method to ensure a correct pole structure.

Another important question in electronic structure calculations for NLO properties is what method to use for larger molecules. While DFT can be used for rather large systems it fails to have the accuracy and systematic behavior of CC theory. In particular problems have been reported for calculations of NLO properties [52, 53, 207, 208]. On the other hand it is unlikely that accurate CC methods including triple excitations like CC3 will become applicable to large systems within the next few years. In recent years the so-called local coupled cluster approach extended successfully the applicability of CC methods for ground state energies to larger molecules. However, the local coupled cluster ansatz faces in its present formulation severe problems when applied in the framework of response theory to excitation energies and to frequency-dependent properties if orbital relaxation has to be treated implicitly through the cluster operator [209, 210]. A complementary approach to reduce the computational costs involves inner projection methods for electron repulsion integrals, as Cholesky decomposition and the resolution-of-the-identity approximation. These have recently been successfully applied for excitation energies and linear response properties at the CC2 level [202, 211]. The operation count for some computational steps can be reduced with inner projection methods by orders of magnitude, but only in special cases the scaling of the costs with system size $\mathcal{N}$ is reduced.

Going beyond the narrow framework of electronic structure theory other major challenges become apparent. The rovibrational contributions to NLO properties are known to be significant. This includes both the vibrational averaging as well as pure (ro)vibrational contributions. The development of general, accurate and efficient methods for the calculation of vibrational contributions is an important area for future research. It requires input from electronic structure calculations and the theoretical interface between electronic and vibrational structure theory is an important issue in this research. For a more detailed discussion we refer to a later Chapter of this book.

Proceeding from the gas to the condensed phase many new issues appear. For NLO properties several additional complications arise when an environment interacts with the system under investigation and external fields need to be considered. Already for the gas phase the proper definition of local field factors and the pressure dependence of (magneto-) optical properties is a difficult issue. In condensed phase, an important question is the proper definition of solute properties and the solvent effect for the electronic property itself. We refer the reader to a comprehensive discussion of solvent effects on NLO properties in a later Chapter. Some of the schemes for modeling solvent effect have been employed in connection with calculation of electronic NLO properties, also recently at the CC level [212,213]. This is still an area where much progress is expected in the coming years.

Acknowledgements

The authors acknowledge support from the EU training and research network NANOQUANT ("Understanding Nanomaterials from a Quantum Perspective", contract No. MRTN-CT-2003-506842), the Deutsche Forschungsgemeinschaft, the Fonds der Chemischen Industrie, the Danish Research Agency, and the Danish Center for Scientific Computing. Many thanks are also due to the long list of collaborators who contributed over many years to the work reviewed here.

References

[1] J. F. Ward and C. K. Miller, Phys. Rev. A. **19**, 826 (1979).

[2] V. Mizrahi and D. P. Shelton, Phys. Rev. Letters. **55**, 696 (1985).

[3] V. Mizrahi and D. P. Shelton, Phys. Rev. A. **31**, 3145 (1985).

[4] D. P. Shelton and V. Mizrahi, Phys. Rev. A. **33**, 72 (1986).

[5] V. Mizrahi and D. P. Shelton, Phys. Rev. A. **33**, 1396 (1986).

[6] D. P. Shelton, Phys. Rev. A. **42**, 2578 (1990).

[7] J. Dudley and J. Ward, J. Chem. Phys. **82**, 4673 (1985).

[8] H. Sekino and R. J. Bartlett, J. Chem. Phys. **98**, 3022 (1993).

[9] P. R. Taylor, T. J. Lee, J. E. Rice and J. Almlöf, Chem. Phys. Lett. **163**, 359 (1989).

[10] G. Maroulis and A. J. Thakkar, Chem. Phys. Lett. **156**, 87 (1989).

[11] J. E. Rice, P. R. Taylor, T. J. Lee and J. Almlöf, J. Chem. Phys. **94**, 4972 (1991).

[12] J. E. Rice, G. E. Scuseria, T. Lee, P. R. Taylor and J. Almlöf, Chem. Phys. Lett. **191**, 23 (1992).

[13] H. Sekino and R. J. Bartlett, J. Chem. Phys. **84**, 2726 (1986).

[14] Y. Luo, H. Ågren, O. Vahtras, P. Jørgensen, V. Spirko and H. Hettema, J. Chem. Phys. **98**, 7159 (1993).

[15] D. M. Bishop, B. Kirtmann, H. A. Kurtz and J. E. Rice, J. Chem. Phys. **98**, 8024 (1993).

[16] D. P. Shelton and J. E. Rice, Chem. Rev. **94**, 3 (1994).

[17] P. Kaatz, E. A. Donley and D. P. Shelton, J. Chem. Phys. **108**, 849 (1998).

[18] D. P. Chong and S. R. Langhoff, J. Chem. Phys. **93**, 570 (1990).

[19] H. J. Å. Jensen, P. Jørgensen, H. Hettema and J. Olsen, Chem. Phys. Lett. **187**, 387 (1991).

[20] Y. Luo, O. Vahtras, H. Ågren and P. Jørgensen, Chem. Phys. Lett. **205**, 555 (1993).

[21] A. D. Buckingham and P. J. Stephens, Ann. Rev. Phys. Chem. **17**, 399 (1966).

[22] P. N. Schatz and A. J. McCaffery, Q. Rev. **23**, 552 (1969).

[23] D. P. Shelton and E. A. Donley, Chem. Phys. Lett. **195**, 591 (1992).

[24] D. M. Bishop, Adv. Quant. Chem. **25**, 1 (1994).

[25] J. E. Rice, J. Chem. Phys. **96**, 7580 (1992).

[26] M. Jaszuński, P. Jørgensen and A. Rizzo, Theor. Chim. Acta. **90**, 291 (1995).

[27] R. J. Bartlett and H. Sekino, in *Non Linear Optical Materials: Theory and Modeling*, edited by S. P. Karna and A. T. Yeates, volume 628 of *American Chemical Society Symposium Series*. American Chemical Society, Washington, 1996.

[28] M. G. Papadopoulos, J. Waite and A. D. Buckingham, J. Chem. Phys. **102**, 371 (1995).

[29] D. P. Shelton and J. J. Palubinskas, J. Chem. Phys. **104**, 2482 (1996).

[30] C. Hättig and P. Jørgensen, Chem. Phys. Lett. **283**, 109 (1998).

[31] P. Rozyczko and R. J. Bartlett, J. Chem. Phys. **107**, 10823 (1997).

[32] C. Hättig and P. Jørgensen, J. Chem. Phys. **109**, 2762 (1998).

[33] R. Franke, H. Müller and J. Noga, J. Chem. Phys. **114**, 7746 (2001).

[34] H. Larsen, J. Olsen, C. Hättig, P. Jørgensen, O. Christiansen and J. Gauss, J. Chem. Phys. **111**, 1917 (1999).

[35] F. Pawłowski, P. Jørgensen and C. Hättig. (2005). to be published.

[36] O. Christiansen, J. Gauss and J. F. Stanton, Chem. Phys. Lett. **305**, 147 (1999).

[37] A. Rizzo, S. Coriani, B. Fernández and O. Christiansen, Phys. Chem. Chem. Phys. **4**, 2884 (2002).

[38] S. Coriani, P. Jørgensen, O. Christiansen and J. Gauss, Chem. Phys. Lett. **330**, 463 (2000).

[39] A. Rizzo, M. Kállay, J. Gauss, F. Pawłowski, P. Jørgensen and C. Hättig, J. Chem. Phys. **121**, 9461 (2004).

[40] A. Rizzo and S. Coriani. Birefringences: a challenge for both theory and experiment. Adv. Quantum Chem., in press.

[41] J. Oddershede. *Propagators Methods*, in *Ab initio Methods in Quantum Chemistry, Part II*, edited by K. P. Lawley, volume 69 of *Adv. Chem. Phys.*, pp. 201–239. John Wiley & Sons, New York, 1987.

[42] J. Olsen and P. Jørgensen. *Time-Dependent Response Theory with Applications to Self-Consistent Field and Multiconfigurational Self-Consistent Field Wave Functions*, in *Modern Electronic Structure Theory*, edited by D. R. Yarkony, volume 2, chapter 13, pp. 857–990. World Scientific, Singapore, 1995.

[43] K. Sasagane, F. Aiga and R. Itoh, J. Chem. Phys. **99**, 3738 (1993).

[44] O. Christiansen, P. Jørgensen and C. Hättig, Int. J. Quantum Chem. **68**, 1 (1998).

[45] P. W. Langhoff, S. T. Epstein and M. Karplus, Rev. Mod. Phys. **44**, 602 (1972).

[46] H. Koch and P. Jørgensen, J. Chem. Phys. **93**, 3333 (1990).

[47] J. F. Stanton and R. J. Bartlett, J. Chem. Phys. **98**, 7029 (1993).

[48] C. Hättig and B. A. Heß, Chem. Phys. Lett. **233**, 359 (1995).

[49] D. L. Yeager and P. Jørgensen, Chem. Phys. Lett. **65**, 77 (1979).

[50] P. Jørgensen, H. J. A. Jensen and J. Olsen, J. Chem. Phys. **89**, 3654 (1988).

[51] E. Dalgaard and H. J. Monkhorst, Phys. Rev. A. **28**, 1217 (1983).

[52] S. J. A. van Gisbergen, J. G. Snijders and E. J. Baerends, J. Chem. Phys. **109**, 10644 (1998).

[53] P. Sałek, O. Vahtras, T. Helgaker and H. Ågren, J. Chem. Phys. **117**, 9630 (2002).

[54] K. Raghavachari, G. W. Trucks, J. A. Pople and M. Head-Gordon, Chem. Phys. Lett. **157**, 479 (1989).

[55] H. Koch, O. Christiansen, P. Jørgensen and J. Olsen, Chem. Phys. Lett. **244**, 75 (1995).

[56] H. Koch, O. Christiansen, P. Jørgensen, A. Sánchez de Merás and T. Helgaker, J. Chem. Phys. **106**, 1808 (1997).

[57] O. Christiansen, H. Koch and P. Jørgensen, Chem. Phys. Lett. **243**, 409 (1995).

[58] O. Christiansen, H. Koch and P. Jørgensen, J. Chem. Phys. **103**, 7429 (1995).

[59] O. Christiansen. *A hierachy of coupled cluster models for accurate calculations of molecular properties*. Ph.D. Thesis, University of Aarhus, 1997.

[60] R. Kobayashi, H. Koch and P. Jørgensen, Chem. Phys. Lett. **219**, 30 (1994).

[61] O. Christiansen, A. Halkier, H. Koch, P. Jørgensen and T. Helgaker, J. Chem. Phys. **108**, 2801 (1998).

[62] O. Christiansen, J. Gauss and J. F. Stanton, Chem. Phys. Lett. **292**, 437 (1998).

[63] K. Hald, F. Pawłowski, P. Jørgensen and C. Hättig, J. Chem. Phys. **118**, 1292 (2003).

[64] M. Kállay and J. Gauss. To be published.

[65] C. Hättig, O. Christiansen, H. Koch and P. Jørgensen, Chem. Phys. Lett. **269**, 428 (1997).

[66] J. Gauss, O. Christiansen and J. F. Stanton, Chem. Phys. Lett. **296**, 117 (1998).

[67] F. Pawłowski. *Development and implementation of CC3 response theory for calculation of frequency-dependent molecular properties. Benchmarking of static molecular properties*. Ph.D. Thesis, University of Aarhus, 2004.

[68] C. Hättig, O. Christiansen and P. Jørgensen, Chem. Phys. Lett. **282**, 139 (1998).

[69] K. Hald. *Molecular properties in Coupled-Cluster theory*. Ph.D. Thesis, University of Aarhus, 2002.

[70] S. Coriani. *Ab initio determination of molecular properties*. Ph.D. Thesis, University of Aarhus, 2000.

[71] S. Coriani, C. Hättig, P. Jørgensen and T. Helgaker, J. Chem. Phys. **113**, 3561 (2000).

[72] G. D. Purvis III and R. J. Bartlett, J. Chem. Phys. **76**, 1910 (1982).

[73] F. Pawłowski, P. Jørgensen and C. Hättig, Chem. Phys. Lett. **391**, 27 (2004).

[74] S. Coriani, C. Hättig, P. Jørgensen, A. Halkier and A. Rizzo, Chem. Phys. Lett. **281**, 445 (1997). Erratum, ibid. **293** (1998) 324.

[75] C. Hättig, O. Christiansen and P. Jørgensen, J. Chem. Phys. **108**, 8355 (1998).

[76] C. L. Thomsen, D. Madsen, S. R. Keiding, J. Thogersen and O. Christiansen, J. Chem. Phys. **110**, 3453 (1999).

[77] H. Koch and R. J. Harrison, J. Chem. Phys. **95**, 7479 (1991).

[78] H. Larsen, C. Hättig, J. Olsen and P. Jørgensen, Chem. Phys. Lett. **291**, 536 (1998).

[79] T. Helgaker, P. Jørgensen and J. Olsen. *Molecular Electronic-Structure Theory*. John Wiley & Sons, New York, 2000.

[80] M. Urban, J. Noga, S. J. Cole and R. J. Bartlett, J. Chem. Phys. **83**, 4041 (1985).

[81] J. Noga, R. J. Bartlett and M. Urban, Chem. Phys. Lett. **134**, 126 (1987).

[82] S. A. Kucharski and R. J. Bartlett, J. Chem. Phys. **108**, 9221 (1998).

[83] Y. S. Lee and R. J. Bartlett, J. Chem. Phys. **80**, 4371 (1984).

[84] Y. S. Lee, S. A. Kucharski and R. J. Bartlett, J. Chem. Phys. **81**, 5906 (1984).

[85] J. Gauss, in *The Encyclopedia of Computational Chemistry*, edited by P. von Ragué Schleyer. John Wiley & Sons, New York, 1998.

[86] edited by R. J. Bartlett. *Recent Advances in Coupled-Cluster Methods*. World Scientific, Singapore, 1997.

[87] R. J. Bartlett. *Coupled-Cluster Theory: An Overview of Recent Developments*, in *Modern Electronic Structure Theory*, edited by D. R. Yarkony, volume 2, chapter 16, pp. 1047–1131. World Scientific, Singapore, 1995.

[88] W. Kutzelnigg, Theor. Chim. Acta. **83**, 263 (1992).

[89] J. E. Rice and N. C. Handy, J. Chem. Phys. **94**, 4959 (1991).

[90] H. Sambe, Phys. Rev. A. **7**, 2203 (1973).

[91] J. Olsen and P. Jørgensen, J. Chem. Phys. **82**, 3235 (1985).

[92] T. B. Pedersen and H. Koch, J. Chem. Phys. **106**, 8059 (1997).

[93] T. Helgaker and P. Jørgensen, Calculation of geometrical derivatives in molecular electronic structure theory, in *Methods in Computational Physics*, edited by S. Wilson and G. H. F. Diercksen, pp. 513–421. Plenum Press, New York, 1992.

[94] P. Kramer and M. Saraceno. *Geometry of the Time-Dependent Variatonal Principle in Quantum Mechanics*. Number 140 in Lecture Notes in Physics. Springer-Verlag, Berlin, 1981.

[95] C. Hättig, O. Christiansen and P. Jørgensen, J. Chem. Phys. **108**, 8331 (1998).

[96] P. N. Butcher and D. Cotter. *The Elements of Nonlinear Optics*. Cambridge University, Cambridge, 1990.

[97] R. K. Nesbet, Phys. Rev. A. **16**, 1 (1977).

[98] F. Visser, P. E. S. Wormer and W. P. J. H. Jacobs, J. Chem. Phys. **82**, 3753 (1985).

[99] P. E. S. Wormer and W. Rijks, Phys. Rev. A. **33**, 2928 (1986).

[100] D. Spelsberg, T. Lorenz and W. Meyer, J. Chem. Phys. **99**, 7845 (1993).

[101] O. Christiansen, C. Hättig and J. Gauss, J. Chem. Phys. **109**, 4745 (1998).

[102] E. A. Salter, H. Sekino and R. J. Bartlett, J. Chem. Phys. **87**, 502 (1987).

[103] R. Kobayashi, H. Koch, P. Jørgensen and T. J. Lee, Chem. Phys. Lett. **211**, 94 (1993).

[104] F. London, J. Phys. Radium. **8**, 397 (1937).

[105] H. F. Hameka, Mol. Phys. **1**, 203 (1958).

[106] R. Ditchfield, J. Chem. Phys. **56**, 5688 (1972).

[107] R. Ditchfield, Mol. Phys. **27**, 789 (1974).

[108] T. Helgaker and P. Jørgensen, J. Chem. Phys. **95**, 2595 (1991).

[109] K. L. Bak, J. Gauss, P. Jørgensen, J. Olsen, T. Helgaker and J. F. Stanton, J. Chem. Phys. **114**, 6548 (2001).

[110] K. L. Bak, P. Jørgensen, J. Olsen, T. Helgaker and W. Klopper, J. Chem. Phys. **112**, 9229 (2000).

[111] K. L. Bak, A. Halkier, P. Jørgensen, J. Olsen, T. Helgaker and W. Klopper, J. Mol. Struct. **567**, 375 (2001).

[112] J. M. L. Martin, J. Chem. Phys. **100**, 8186 (1994).

[113] T. A. Ruden, T. Helgaker, P. Jørgensen and J. Olsen, J. Chem. Phys. **121**, 5874 (2004).

[114] A. A. Auer, J. Gauss and J. F. Stanton, J. Chem. Phys. **118**, 10407 (2003).

[115] J. F. Stanton, J. Gauss, J. D. Watts, W. J. Lauderdale and R. J. Bartlett. ACES II. Quantum Theory Project, University of Florida, Gainesville, Florida. See also J. F. Stanton, J. Gauss, J. D. Watts, W. J. Lauderdale, R. J. Bartlett, *Int J. Quantum Chem.* **S26**, 879, (1992). ACES II uses the VMOL integral and the VPROPS property integral programs written by J. Almlöf and P. R. Taylor, a modified version of the integral derivative program ABACUS written by T. Helgaker, H. J. Aa. Jensen, P. Jørgensen, J. Olsen, and P. R. Taylor, and a geometry optimization and vibrational analysis package written by J. F. Stanton and D. E. Bernholdt. See also `http://www.aces2.de` for further information.

[116] H. Koch, A. Sánchez de Merás, T. Helgaker and O. Christiansen, J. Chem. Phys. **104**, 4157 (1996).

[117] H. Koch, O. Christiansen, R. Kobayashi, P. Jørgensen and T. Helgaker, Chem. Phys. Lett. **228**, 233 (1994).

[118] T. Helgaker, H. J. Å. Jensen, P. Jørgensen, J. Olsen, K. Ruud, H. Ågren, A. A. Auer, K. L. Bak, V. Bakken, O. Christiansen, S. Coriani, P. Dahle, E. K. Dalskov, T. Enevoldsen, B. Fernandez, C. Hättig, K. Hald, A. Halkier, H. Heiberg, H. Hettema, D. Jonsson, S. Kirpekar, R. Kobayashi, H. Koch, K. V. Mikkelsen, P. Norman, M. J. Packer, T. B. Pedersen, T. A. Ruden, A. Sanchez, T. Saue, S. P. A. Sauer, B. Schimmelpfennig, K. O. Sylvester-Hvid, P. R.Taylor, and O.Vahtras. DALTON – an electronic structure program, release 1.2, 2001.

[119] C. Hättig. *Coupled-Cluster-Methoden zur Berechnung nichtlinearer optischer Eigenschaften und angeregter Zustände von Molekülen*. Habil. Thesis, University of Karlsruhe, 2003.

[120] T. H. Dunning, J. Chem. Phys. **90**, 1007 (1989).

[121] R. A. Kendall, T. H. Dunning and R. J. Harrison, J. Chem. Phys. **96**, 6796 (1992).

[122] D. E. Woon and T. H. Dunning, J. Chem. Phys. **98**, 1358 (1993).

[123] D. E. Woon and T. H. Dunning, J. Chem. Phys. **100**, 2975 (1994).

[124] C. Hättig, H. Koch and P. Jørgensen, J. Chem. Phys. **109**, 3293 (1998).

[125] S. Høst, P. Jørgensen, A. Köhn, F. Pawłowski, W. Klopper and C. Hättig. (2005). to be published.

[126] H. Koch, R. Kobayashi and P. Jørgensen, Int. J. Quantum Chem. **49**, 835 (1994).

[127] F. Aiga, K. Sasagane and R. Itoh, Int. J. Quantum Chem. **51**, 87 (1994).

[128] O. Christiansen, H. Koch, P. Jørgensen and J. Olsen, Chem. Phys. Lett. **256**, 185 (1996).

[129] H. Larsen, K. Hald, J. Olsen and P. Jørgensen, J. Chem. Phys. **115**, 3015 (2001).

[130] H. Larsen, J. Olsen, P. Jørgensen and O. Christiansen, J. Chem. Phys. **113**, 6677 (2000). Erratum ibid. **114** (2001) 10985.

[131] W. Klopper, S. Coriani, T. Helgaker and P. Jørgensen, J. Phys. B. **37**, 3753 (2004).

[132] P. J. Stephens, Ann. Rev. Phys. Chem. **25**, 201 (1974).

[133] P. J. Stephens, Adv. Chem. Phys. **35**, 197 (1976).

[134] A. D. Buckingham, J. Chem. Phys. **30**, 1580 (1959).

[135] A. D. Buckingham and H. C. Longuet-Higgins, Mol. Phys. **14**, 63 (1968).

[136] A. Cotton and M. Mouton, Compt. Rend. **141**, 317 (1905).

[137] A. D. Buckingham and J. A. Pople, Proc. Phys. Soc. B. **69**, 1133 (1956).

[138] J. Kerr, Phil. Mag. **4 (50)**, 337 (1875).

[139] J. Kerr, Phil. Mag. **4 (50)**, 416 (1875).

[140] R. C. Jones, J. Opt. Soc. Am. **38**, 671 (1948).

[141] E. B. Graham and R. E. Raab, Proc. R. Soc. Lond. A. **390**, 73 (1983).

[142] F. Pockels, Radium. **10**, 152 (1913).

[143] E. B. Graham and R. E. Raab, Mol. Phys. **52**, 1241 (1984).

[144] K. Wolinski, J. Hinton and P. Pulay, J. Am. Chem. Soc. **112**, 8251 (1990).

[145] M. Faraday, Philos. Mag. **28**, 294 (1846).

[146] M. Faraday, Philos. Trans. R. Soc. London. **136**, 1 (1846).

[147] E. M. Verdet, Ann. Chimie (3rd Ser.). **41**, 370 (1854).

[148] P. A. Snyder, R. W. C. Hansen and E. M. Rowe, J. Phys. Chem. **100**, 17756 (1996).

[149] S. Coriani, C. Hättig and A. Rizzo, J. Chem. Phys. **111**, 7828 (1999).

[150] D. M. Bishop and S. M. Cybulski, J. Chem. Phys. **93**, 590 (1990).

[151] L. R. Ingersoll and D. H. Liebenberg, J. Opt. Soc. Am. **46**, 538 (1956).

[152] D. M. Bishop and S. P. A. Sauer, J. Chem. Phys. **107**, 8502 (1997).

[153] K. Ruud, P.-O. Åstrand and P. R. Taylor, J. Chem. Phys. **112**, 2668 (2000).

[154] J. Stanton, Mol. Phys. **97**, 841 (1999).

[155] D. L. Gray and A. G. Robiette, Mol. Phys. **37**, 1901 (1979).

[156] J. Herranz and B. P. Stoicheff, J. Mol. Spectr. **10**, 448 (1963).

[157] J. Gauss and J. Stanton, Adv. Chem. Phys. **123**, 355 (2003).

[158] D. A. Imrie and R. E. Raab, Mol. Phys. **74**, 833 (1991).

[159] S. Coriani, A. Halkier and A. Rizzo, The electric-field-gradient-induced birefringence and the determination of molecular quadrupole moments, in *Recent Research Developments in Chemical Physics, Vol. 2,* pg. 1, edited by G. Pandalai. Transworld Scientific, Kerala, India, 2001.

[160] A. D. Buckingham and M. J. Jamieson, Mol. Phys. **22**, 117 (1971).

[161] S. Coriani, C. Hättig, P. Jørgensen, A. Rizzo and K. Ruud, J. Chem. Phys. **109**, 7176 (1998).

[162] S. Coriani, A. Halkier, A. Rizzo and K. Ruud, Chem. Phys. Lett. **326**, 269 (2000).

[163] C. Cappelli, U. Ekström, A. Rizzo and S. Coriani, J. Comp. Meth. Sci. Eng. (JCMSE). **4**, 365 (2004).

[164] A. Rizzo, S. Coriani, A. Halkier and C. Hättig, J. Chem. Phys. **113**, 3077 (2000).

[165] S. Coriani, A. Halkier, D. Jonsson, J. Gauss, A. Rizzo and O. Christiansen, J. Chem. Phys. **118**, 7329 (2003).

[166] A. J. Russell and M. A. Spackman, Mol. Phys. **88**, 1109 (1996).

[167] C. Graham, D. A. Imrie and R. E. Raab, Mol. Phys. **93**, 49 (1998).

[168] A. D. Buckingham and R. L. Disch, Proc. Roy. Soc. A. **273**, 275 (1963).

[169] A. Halkier, S. Coriani and P. Jørgensen, Chem. Phys. Lett. **294**, 292 (1998).

[170] G. L. D. Ritchie, J. N. Watson and R. I. Keir, Chem. Phys. Lett. **370**, 376 (2003).

[171] A. Halkier and S. Coriani, Chem. Phys. Lett. **303**, 408 (1999).

[172] J. N. Watson, I. E. Craven and G. L. D. Ritchie, Chem. Phys. Lett. **274**, 1 (1997).

[173] R. I. Keir, D. W. Lamb, G. L. D. Ritchie and J. N. Watson, Chem. Phys. Lett. **279**, 22 (1997).

[174] M. R. Battaglia, A. D. Buckingham, D. Neumark, R. K. Pierens and J. H. Williams, Mol. Phys. **43**, 1015 (1981).

[175] G. L. D. Ritchie, Field-gradient induced birefringence: a direct route to molecular quadrupole moments, in *Optical, Electric and Magnetic Properties of Molecules,* pg. 67, edited by D. C. Clary and B. Orr. Elsevier, Amsterdam, The Netherlands, 1997.

[176] A. D. Buckingham, R. L. Disch and D. A. Dunmur, J. Am. Chem. Soc. **90**, 3104 (1968).

[177] O. L. de Lange and R. E. Raab, Mol. Phys. **102**, 125 (2004).

[178] R. E. Raab and O. L. de Lange, Mol. Phys. **101**, 3467 (2003).

[179] C. Rizzo, A. Rizzo and D. M. Bishop, Int. Rev. Phys. Chem. **16**, 81 (1997).

[180] A. Rizzo and C. Rizzo, Mol. Phys. **96**, 973 (1999).

[181] K. Muroo, N. Ninomiya, M. Yoshino and Y. Takubo, J. Opt. Soc. Am. B. **20**, 2249 (2003).

[182] R. Cameron, G. Cantatore, A. C. Melissinos, J. Rogers, Y. Semertzidis, H. Halama, A. Prodell, F. A. Nezrick, C. Rizzo, and E. Zavattini, J. Opt. Soc. Am. B. **8**, 520 (1991).

[183] S. Carusotto, E. Iacopini, E. Polacco, F. Scuri, G. Stefanini and E. Zavattini, J. Opt. Soc. Am. B. **1**, 635 (1984).

[184] A. Rizzo and S. Coriani, J. Chem. Phys. **119**, 11064 (2003).

[185] F. Pawłowski, P. Jørgensen, A. Rizzo and C. Hättig. to be published.

[186] G. L. J. A. Rikken, E. Raupach and T. Roth, Physica B. **294-295**, 1 (2001).

[187] T. Roth and G. L. J. A. Rikken, Phys. Rev. Lett. **85**, 4478 (2000).

[188] T. Roth. Experimental verification of the Jones birefringence induced in liquids. Diploma thesis, Darmstadt University of Technology and Grenoble High Magnetic Field Laboratory, 2000.

[189] A. Rizzo, C. Cappelli, B. Jansík, D. Jonsson, P. Sałek, S. Coriani and H. Ågren, J. Chem. Phys. **121**, 8814 (2004).

[190] A. Rizzo, C. Cappelli, B. Jansík, D. Jonsson, P. Sałek, S. Coriani, D. J. D. Wilson, T. Helgaker and H. Ågren, Phys. Chem. Chem. Phys. (2005). submitted.

[191] H. Koch, H. J. A. Jensen, P. Jørgensen and T. Helgaker, J. Chem. Phys. **93**, 3345 (1990).

[192] O. Christiansen, H. Koch, A. Halkier, P. Jørgensen, T. Helgaker and A. M. Sánchez de Merás, J. Chem. Phys. **105**, 6921 (1996).

[193] O. Christiansen, H. Koch, P. Jørgensen and T. Helgaker, Chem. Phys. Lett. **263**, 530 (1996).

[194] H. Koch, R. Kobayashi, A. Sánchez de Merás and P. Jørgensen, J. Chem. Phys. **100**, 4393 (1994).

[195] B. Datta, P. Sen and D. Mukherjee, J. Phys. Chem. **99**, 6441 (1995).

[196] J. F. Stanton and R. J. Bartlett, J. Chem. Phys. **99**, 5178 (1993).

[197] K. Hald, P. Jørgensen, J. Olsen and M. Jaszuński, J. Chem. Phys. **115**, 671 (2001).

[198] J. F. Stanton and J. Gauss, J. Chem. Phys. **100**, 4695 (1994).

[199] S. R. Gwaltney and R. J. Bartlett, J. Chem. Phys. **110**, 62 (1999).

[200] M. Nooijen and R. J. Bartlett, J. Chem. Phys. **102**, 3629 (1995).

[201] J. D. Watts and R. J. Bartlett, Chem. Phys. Lett. **233**, 81 (1995).

[202] C. Hättig and F. Weigend, J. Chem. Phys. **113**, 5154 (2000).

[203] P. Rozyczko, S. A. Perera, M. Nooijen and R. J. Bartlett, J. Chem. Phys. **107**, 6736 (1997).

[204] C. E. Smith, R. A. King and T. D. Crawford, J. Chem. Phys. **122**, 054110 (2004).

[205] P. Sałek, T. Helgaker and T. Saue, Chem. Phys. **311**, 187 (2005).

[206] P. Norman, B. Schimmelpfenning, K. Ruud, H. J. A. Jensen and H. Ågren, J. Chem. Phys. **116**, 6914 (2002).

[207] Z. L. Cai, K. Sendt and J. R. Reimers, J. Chem. Phys. **117**, 5543 (2002).

[208] P. Sałek, T. Helgaker, O. Vahtras, H. Ågren, D. Jonsson and J. Gauss, Mol. Phys. **103**, 439 (2005).

[209] T. Korona, K. Pflüger and H.-J. Werner, Phys. Chem. Chem. Phys. **6**, 2059 (2004).

[210] N. Russ and T. Crawford, Chem. Phys. Lett. **400**, 104 (2004).

[211] T. B. Pedersen, A. M. Sánchez de Merás and H. Koch, J. Chem. Phys. **120**, 8887 (2004).

[212] J. Kongsted, A. Osted, K. V. Mikkelsen and O. Christiansen, J. Chem. Phys. **119**, 10519 (2003).

[213] J. Kongsted, A. Osted, K. V. Mikkelsen and O. Christiansen, J. Chem. Phys. **120**, 3787 (2004).